




Two-detector flavor sensitivity to ultra-high-energy cosmic neutrinos

Federico Testagrossa ^{1,*} Damiano F. G. Fiorillo ^{2,†} and Mauricio Bustamante ^{2,‡}

¹*Dipartimento di Fisica e Astronomia, Università di Padova, Via Marzolo 8, 35131 Padova, Italy*

²*Niels Bohr International Academy, Niels Bohr Institute,*

University of Copenhagen, 2100 Copenhagen, Denmark

(Dated: October 18, 2023)

Ultra-high-energy (UHE) cosmic neutrinos, with energies above 100 PeV, could be finally discovered in the near future. Measuring their flavor composition would reveal information about their production and propagation, but new techniques are needed for UHE neutrino telescopes to have the capabilities to do it. We address this by proposing a new way to measure the UHE neutrino flavor composition that does not rely on individual telescopes having flavor-identification capabilities. We manufacture flavor sensitivity from the joint detection by one telescope sensitive to all flavors—the radio array of IceCube-Gen2—and one mostly sensitive to ν_τ —GRAND. From this limited flavor sensitivity, predominantly to ν_τ , and even under conservative choices of neutrino flux and detector size, we extract important insight. For astrophysics, we forecast meaningful constraints on the neutrino production mechanism; for fundamental physics, vastly improved constraints on Lorentz-invariance violation. These are the first measurement forecasts of the UHE ν_τ content.

I. INTRODUCTION

High-energy cosmic neutrinos are incisive probes of extreme astrophysics and fundamental physics. For astrophysics, they address the long-standing question of the origin of ultra-high-energy cosmic rays (UHECRs) [1–10]. For fundamental physics, they probe the highest neutrino energy scales, otherwise unreachable, where new physics may manifest [8, 9, 11–14]. On both fronts, their flavor composition, i.e., the proportion of neutrinos of different flavor, ν_e , ν_μ , and ν_τ , in their flux is a particularly versatile observable [15–67].

Today, the IceCube neutrino telescope regularly detects high-energy astrophysical neutrinos of 10 TeV–10 PeV, the most energetic ones seen so far [68–75]. They have already delivered valuable new insight, including via their flavor composition [71, 76–82]. Beyond them, long-foretold ultra-high-energy (UHE) neutrinos [83], with energies larger than 100 PeV, hold the potential to deliver even more. Yet, so far, they remain undiscovered [84, 85]: their flux, although unknown, is likely too low to be seen by existing detectors [4, 9]. Fortunately, in the next decade, a host of new planned detectors [4, 9, 10, 86] will have a realistic chance of discovering UHE neutrinos even if their flux is tiny [87–91].

However, the measurement of the flavor composition of UHE neutrinos has received little attention, the focus being instead on first establishing the discovery potential of the planned detectors; see, e.g., Refs. [87–89, 91]. Further, because they use detection strategies different [9, 86] from optical-light detection at IceCube [92]—i.e., radio in-ice [93, 94] and in-air [95–100], Cherenkov light [101, 102]—new techniques are needed to distinguish between similar signals made by neutrinos of different flavor. For in-ice radio-based detection, there are promising prospects [103–106].

We sideline this challenge by proposing a new way to measure the UHE neutrino flavor composition that bypasses the need for individual detectors to have flavor-

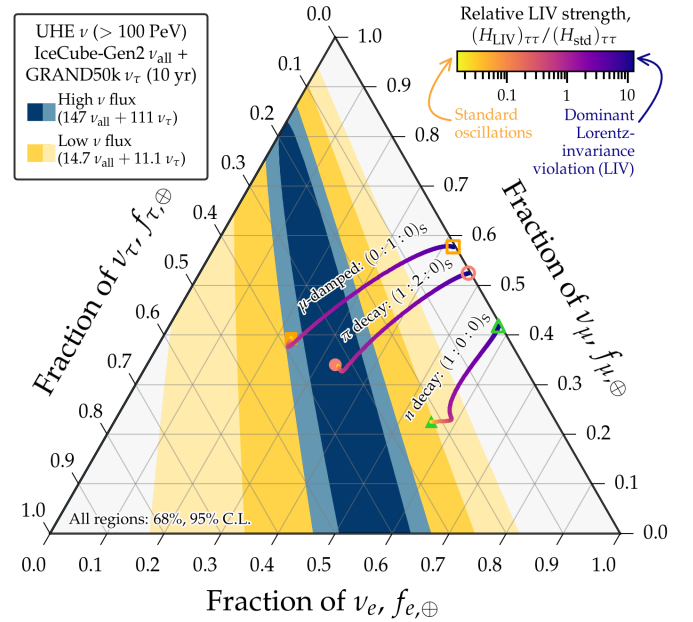


FIG. 1. *Projected measurement of the flavor composition of ultra-high-energy neutrinos.* The regions of allowed flavor composition, obtained by combining measurements of neutrinos of all flavors in the radio array of IceCube-Gen2 [107] and of ν_τ in GRAND50k [96], assuming high and low benchmark neutrino flux models. Overlaid is the flavor composition at the Earth under standard oscillations and in the presence of Lorentz-invariance violation (LIV) of varying strength, for three benchmarks of the flavor composition at the neutrino sources.

identification capabilities. Instead, we exploit the synergy between different detection strategies.

We manufacture flavor sensitivity from the combined action of two planned detectors: one that detects all neutrino flavors roughly indistinctly—e.g., the planned radio

array of IceCube-Gen2—and one that detects predominantly ν_τ —e.g., GRAND. This allows us to measure the fraction of ν_τ in the diffuse UHE flux.

Figure 1 shows, for the first time, that this measurement is possible, even under conservative assumptions: a relatively low UHE neutrino flux and an intermediate-size configuration of GRAND. Even this limited measurement, of a single flavor fraction, affords important new insight into neutrino astrophysics and fundamental physics. For astrophysics, it allows us to infer the flavor composition with which the neutrinos were produced, which helps identify their production process and sources (Fig. 3). For fundamental physics, it allows us to improve constraints of physics beyond the Standard Model by many orders of magnitude (Fig. 4).

The rest of the paper is structured as follows. In Sec. II we introduce the main features of UHE neutrinos and their flavor composition. In Sec. III we characterize the detector response and show how the event rates in each experiment are computed. In Sec. IV we introduce the statistical analysis used to measure the flavor composition. In Sec. IV A, we show our results on astrophysics. In Sec. V, we show our results on fundamental physics. In Sec. VI, we summarize and conclude.

II. UHE NEUTRINO FLUXES

In the 1960s, it was realized that the existence of UHE neutrinos, above 100 PeV, could be expected on general grounds [83]. UHECR protons with energies above 10^{12} GeV propagating in extragalactic space should interact with the cosmic microwave background, producing UHE *cosmogenic* neutrinos of comparable energies [108, 109]. UHECRs could also interact with matter or radiation inside their sources, yielding *astrophysical* UHE neutrinos [110–140]. UHE neutrinos may reach the Earth after traveling Gpc-scale distances undeterred by matter or radiation, their energies dampened only mildly by the adiabatic cosmological expansion. Thus, they are direct probes of UHECRs and of processes at ultra-high energies.

Today, UHE neutrinos remain undetected. Predictions of the size and shape of their flux are uncertain [74, 75, 116, 118, 130, 141–151] because they rely on uncertainly known properties of UHECRs—their mass composition, maximum energies, and shape of their energy spectrum—and of their unknown sources—mainly, their abundance at different redshifts [3, 8]. Broadly stated, light UHECR mass composition, low maximum energies, a spectrum that falls slowly with energy, and an abundance of distant sources yield higher UHE neutrino fluxes; changes in each of these factors in the opposite direction yield lower fluxes; see, e.g., Refs. [142, 146–148]. Figure 5 in Ref. [87] and Fig. 2 in Ref. [89] illustrate the present-day breadth of predictions of the diffuse UHE neutrino flux. Our choice of benchmark for the diffuse flux introduced below, in Eq. (1), is motivated by them.

A. Energy spectrum

Since our purpose is to measure the flavor composition of UHE neutrinos, what matters is their energy distribution, which determines how many we can expect to detect. Thus, in lieu of detailed flux modeling, we adopt for the neutrino energy spectrum a heuristic shape that captures the essential features of many predictions. For the diffuse flux of UHE $\nu_\alpha + \bar{\nu}_\alpha$ ($\alpha = e, \mu, \tau$), this is [152]

$$E_\nu^2 \Phi_\alpha = \Phi_0 f_{\alpha,\oplus} \exp \left[-w \log^2 \left(\frac{E_\nu}{E_{\text{bump}}} \right) \right], \quad (1)$$

i.e., a log-parabola with height Φ_0 , width w , and centered at energy E_{bump} , that captures the bump-like feature in the neutrino spectrum expected in production via proton-photon interactions [123, 153–156]. For the flavor composition at Earth, $f_{\alpha,\oplus}$, we adopt the expectation from pion decay (see Sec. II B).

As benchmark, we adopt for Φ_0 , w , and E_{bump} values that yields an all-flavor flux, $\sum_\alpha \Phi_\alpha$ from Eq. (1), that approximates the predicted neutrino flux from newborn pulsars, from Ref. [130], which peaks at $\sim 3 \cdot 10^8$ GeV, and is representative of the breadth in predictions. We compare predictions made with this flux (“high”) *vs.* predictions made with a flux ten times smaller (“low”). They yield, respectively, ~ 100 and ~ 10 events in 10 years in IceCube-Gen2 and GRAND50k (see Sec. III A).

B. Flavor composition

UHECR interactions produce high-energy pions that, upon decaying, make high-energy neutrinos, i.e., $\pi^+ \rightarrow \mu^+ + \nu_\mu$ followed by $\mu^+ \rightarrow \bar{\nu}_\mu + e^+ + \nu_e$, and their charge-conjugated processes. Thus, the full pion decay chain yields a flavor composition at the sources (S) of $(f_{e,S}, f_{\mu,S}, f_{\tau,S}) = (\frac{1}{3}, \frac{2}{3}, 0)$, where $f_{\alpha,S}$ is the ratio of the flux of $\nu_\alpha + \bar{\nu}_\alpha$ to the total flux emitted. This is our nominal expectation. If the neutrinos are produced in regions that harbor an intense magnetic field, the intermediate muons may cool by synchrotron radiation before decaying, yielding instead $(0, 1, 0)_S$. And, if neutrinos are made in the beta decay of neutrons, we expect only $\bar{\nu}_e$, i.e., $(1, 0, 0)_S$. We consider the above three production scenarios as benchmarks, but pick pion decay to produce our main results.

En route to Earth, neutrinos oscillate; as a result, their flavor composition at the Earth, $f_{\alpha,\oplus}$, is different from that at the sources. For high-energy cosmic neutrinos, because oscillations are rapid and the energy resolution of neutrino telescopes is limited, there is sensitivity only to the average flavor-transition probability. For $\nu_\alpha \rightarrow \nu_\beta$ ($\alpha, \beta = e, \mu, \tau$), this is $P_{\nu_\alpha \rightarrow \nu_\beta} = \sum_i |U_{\alpha i}|^2 |U_{\beta i}|^2$, where the sum is over the three neutrino mass eigenstates, and U is the Pontecorvo-Maki-Nakagawa-Sakata (PMNS) lepton mixing matrix [157, 158], which depends on parameters whose values are known experimentally [159, 160]. For a given flavor composition at

the sources, $f_{\alpha,\oplus} = \sum_{\beta} P_{\nu_{\beta} \rightarrow \nu_{\alpha}} f_{\beta,S}$. Figure 1 shows the expectation for our three benchmarks production scenarios; the nominal expectation, from pion decay, is about $(0.33, 0.34, 0.33)_{\oplus}$.

C. Determining the diffuse neutrino flux

We assume that the diffuse neutrino flux is due to a population of identical, nondescript astrophysical sources distributed in redshift, each of which injects the same neutrino spectrum. The rate of $\nu_{\alpha} + \bar{\nu}_{\alpha}$ emitted per unit energy emitted by an individual source is

$$E_{\nu}^2 \frac{dN_{\alpha}}{dE_{\nu} dt} = C_{\nu} f_{\alpha,S} \exp \left[-w \log^2 \left(\frac{E_{\nu}}{E_{\text{bump}}} \right) \right], \quad (2)$$

which has the same shape as our benchmark diffuse flux, Eq. (1), with C_{ν} a normalization constant (more on it later in this section). The diffuse flux at Earth is the sum of contributions across all redshifts, i.e.,

$$\begin{aligned} \Phi_{\alpha}(E_{\nu}, \tilde{\theta}, \mathbf{f}_S) &= \int \frac{dz}{H(z)} \rho_{\text{src}}(z) \\ &\times \sum_{\beta} \frac{dN_{\alpha}}{dE_{\nu} dt} [E_{\nu}(1+z), \tilde{\theta}, \mathbf{f}_S] P_{\nu_{\beta} \rightarrow \nu_{\alpha}}, \end{aligned} \quad (3)$$

where $\tilde{\theta} \equiv (C_{\nu}, w, E_{\text{bump}})$ are the flux shape parameters, $\mathbf{f}_S \equiv (f_{e,S}, f_{\mu,S}, f_{\tau,S})$ are the flavor fractions at the sources, $H(z) \equiv H_0 [\Omega_{\Lambda} + \Omega_m (1+z)^3]^{1/2}$ is the Hubble parameter, and $\Omega_{\Lambda} = 0.68$ and $\Omega_m = 0.32$ are, respectively, the adimensional energy densities of vacuum and matter [161]. The right-hand side of Eq. (3) is evaluated at an energy $E_{\nu}(1+z)$ to account for the redshifting of the neutrino energy due to the cosmological expansion.

We assume that the number density of the sources, ρ_{src} , follows the star-formation rate, parametrized as in Ref. [162]: $\rho_{\text{src}}(z) = \rho_0 (a + bz) h / [1 + (z/c)^d]$, where $a = 0.017$, $b = 0.13$, $h = 0.7$, $c = 3.3$, $d = 5.3$ for the modified Salpeter initial mass function [163]; the local source density, ρ_0 , is a parameter whose value we do not need to specify explicitly, as we discuss below. This places most of the sources at $z \approx 2$, a few Gpc away; sources at higher redshifts are rarer and contribute little to the diffuse flux.

In Eq. (3), the unknown per-source normalization parameter, C_{ν} , is degenerate with the unknown local density of the sources, ρ_0 . Thus, it is convenient to define an effective normalization parameter, ϕ_0 , with units of flux, via $E_{\nu}^2 \phi_{\alpha} \equiv (\rho_0 / H_0) (dN_{\alpha} / dE_{\nu} dt)$, i.e.,

$$E_{\nu}^2 \phi_{\alpha} = \phi_0 f_{\alpha,S} \exp \left[-w \log^2 \left(\frac{E_{\nu}}{E_{\text{bump}}} \right) \right]. \quad (4)$$

With this, the diffuse flux at Earth becomes

$$\begin{aligned} \Phi_{\alpha}(E_{\nu}, \theta, \mathbf{f}_S) &= \int \frac{dz}{\tilde{H}(z)} \tilde{\rho}_{\text{src}}(z) \\ &\times \sum_{\beta} \phi_{\beta} [E_{\nu}(1+z), \theta, \mathbf{f}_S] P_{\nu_{\beta} \rightarrow \nu_{\alpha}}, \end{aligned} \quad (5)$$

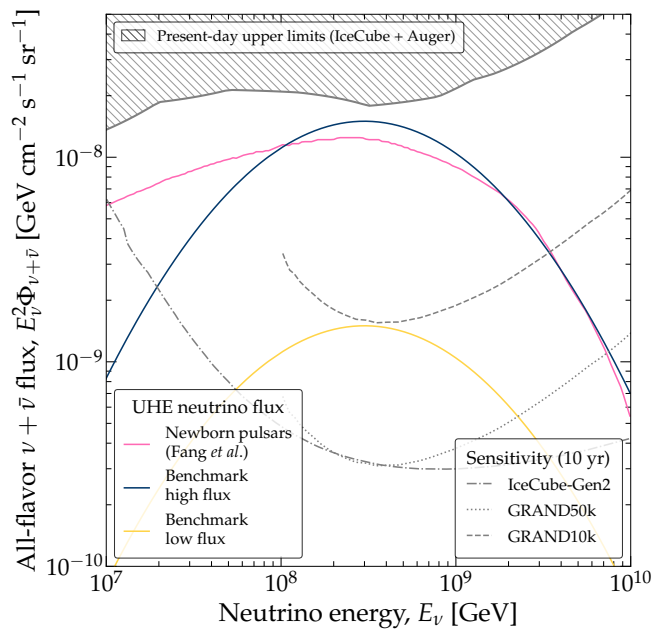


FIG. 2. *UHE neutrino flux benchmark models used in our analysis.* Our benchmark high and low flux models are built from Eq. (1), based off of the predicted flux from newborn pulsars from Ref. [130]. The sensitivity of the radio array of IceCube-Gen2 is from Ref. [107]. The sensitivities of GRAND50k and GRAND10k are computed by inverting Eq. (7), using the effective areas of GRAND50k and GRAND10. The upper limits are from IceCube [84] and Auger [85].

where now the flux parameters are $\theta = (\phi_0, w, E_{\text{bump}})$, $\tilde{\rho}_{\text{src}} = \rho_{\text{src}} / \rho_0$ and $\tilde{H} = H / H_0$. Equations (4) and (5) are the expressions we use in our calculations, and θ are the free parameters that we vary.

We assume neutrino production via pion decay, i.e., $\mathbf{f}_S = (\frac{1}{3}, \frac{2}{3}, 0)$. We fix the normalization of the diffuse flux in Eq. (3) by demanding that the all-flavor flux, $\sum_{\alpha} \Phi_{\alpha}$, approximates our high benchmark flux (Fig. 2). This fixes the shape parameters to $\phi_0 = 2.2 \cdot 10^{-7} \text{ GeV cm}^{-2} \text{ s}^{-1} \text{ sr}^{-1}$, $w = 0.18$, and $E_{\text{bump}} = 5 \cdot 10^8 \text{ GeV}$. To reproduce our low benchmark flux, we use a normalization constant, ϕ_0 , ten times smaller.

Figure 2 shows the all-flavor benchmark UHE diffuse neutrino flux models that we use in our forecasts. They are built using Eq. (1), summed over all flavors. Our high benchmark flux approximates the predicted flux emitted by newborn pulsars from Ref. [130] by computing Eq. (1) with $\Phi_0 = 1.5 \cdot 10^{-8} \text{ GeV cm}^{-2} \text{ s}^{-1} \text{ sr}^{-1}$, $w = 0.25$, and $E_{\text{bump}} = 3 \cdot 10^8 \text{ GeV}$. The low flux has a normalization, Φ_0 , ten times smaller. We use the flux shape given by Eq. (1) rather than directly the prediction of Ref. [130] because doing so allows us to account for uncertainties in the flux shape by varying α and E_{bump} . For details about our choice of spectrum in Eq. (1), see Ref. [152].

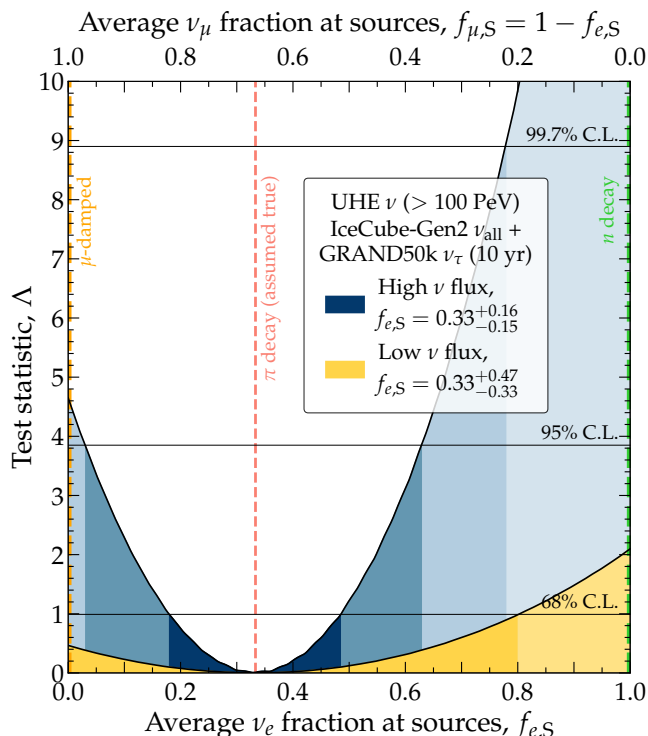


FIG. 3. *Inferred flavor composition of UHE cosmic neutrinos at their sources.* The results are projections obtained from measuring the fraction $f_{\tau,\oplus}$ of ν_τ at Earth by combining the detection by the radio array of IceCube-Gen2 and GRAND50k (Fig. 1), using methods from Refs. [61, 66]. We assume neutrino production via pion decay, no ν_τ production (i.e., $f_{\tau,S} = 0$), and two benchmark UHE neutrino fluxes, high and low.

III. DETECTING UHE NEUTRINOS

IceCube-Gen2 [93] and GRAND [96] target the radio-detection of UHE neutrinos [166]. While they share common features, i.e., they are both affected by the severe attenuation of the UHE neutrino flux inside Earth and both exploit the long attenuation length of radio in ice and air, they adopt different, complementary strategies. Below, we outline them.

The radio array of IceCube-Gen2 looks for radio signals in-ice, emitted by particle showers triggered by UHE neutrinos scattering off nucleons [81, 167–169]. The showers accrue an excess of electrons that is discharged as an Askaryan [170] radio pulse [171, 172] detectable by antennas in the ice. The detection sensitivity is comparable for all neutrino flavors, albeit slightly better for ν_e .

GRAND looks for radio signals above ground, emitted by showers triggered by UHE neutrinos scattering with nucleons just below the surface, including in nearby mountains. This strategy averts a large background of showers triggered instead by UHECRs. GRAND targets predominantly Earth-skimming ν_τ [173], more resilient than ν_e and ν_μ to in-Earth attenuation, whose interac-

tions generate taus that, upon exiting into the air, decay and trigger extensive air showers. The negatively and positively charged particles in them are separated by the geomagnetic field, and the imbalance is discharged as a radio pulse [174] detectable by antennas on the ground.

A. Detector response and event rate computation

We compute the expected rate of detected events after 10 years of exposure, in bins of a quarter of a decade in energy from 10^7 to 10^{10} GeV. For IceCube-Gen2, we sum the contributions from all flavors, based on Refs. [107, 175]; for GRAND, we consider ν_τ only, based on Ref. [96], and ignore potential subdominant contributions from other flavors. We make our predictions conservative by considering only the partial configurations GRAND50k and GRAND10k, which represent one fourth and one tenth of the final size of GRAND, respectively.

In an UHE neutrino detector (det), the differential number of events induced by ν_α of energy E_ν is

$$\frac{dN_\alpha^{\text{det}}}{dE_\nu} = \Omega T \Phi_\alpha A_\alpha^{\text{det}}, \quad (6)$$

where Ω is the solid angle of the sky to which the detector is sensitive, T is the detector exposure time, and A_α^{det} is the effective area of the detector for ν_α . We consider detection in the radio array of IceCube-Gen2 and in GRAND, for an exposure time of 10 years, representative of their design runtimes.

For the radio array of IceCube-Gen2, even though we do not attribute to it flavor-identification capabilities, we compute the contributions of neutrinos of different flavors separately. To this end, we use flavor-specific effective areas, which we build in three steps. First, we infer the flavor-averaged effective area from the differential IceCube-Gen2 sensitivity, $S(E_\nu)$, recently reported by the Collaboration in Ref. [107], i.e.,

$$A_{\text{avg}}^{\text{IC-Gen2}} = \frac{2.44 E_\nu}{\Omega S(E_\nu) T \ln 10}, \quad (7)$$

where the 2.44 events come from using the background-free prescription in the Feldman-Cousins approach [176], and, in this case, $\Omega = 4\pi$ because the sensitivity is reported as all-sky. Second, we pick the flavor-specific effective areas from the `toise` framework [175] (see also Ref. [177]), $A_e^{\text{IC-Gen2}}$, $A_\mu^{\text{IC-Gen2}}$, and $A_\tau^{\text{IC-Gen2}}$ for a benchmark in-ice radio-based neutrino telescope; see Fig. 16 in Ref. [175]. From them, we compute the flavor-averaged effective area, $(\sum_\alpha A_\alpha^{\text{IC-Gen2}})/3$. Third, and finally, we equate this to $A_{\text{avg}}^{\text{IC-Gen2}}$ from Eq. (7) to reweigh the flavor-specific effective areas. Thus, the resulting areas, which we use in our forecasts, reflect both the flavor sensitivity of the detector and its most recent flux-discovery potential. Because we do not ascribe flavor-identification capabilities to the radio array of IceCube-Gen2, we use the

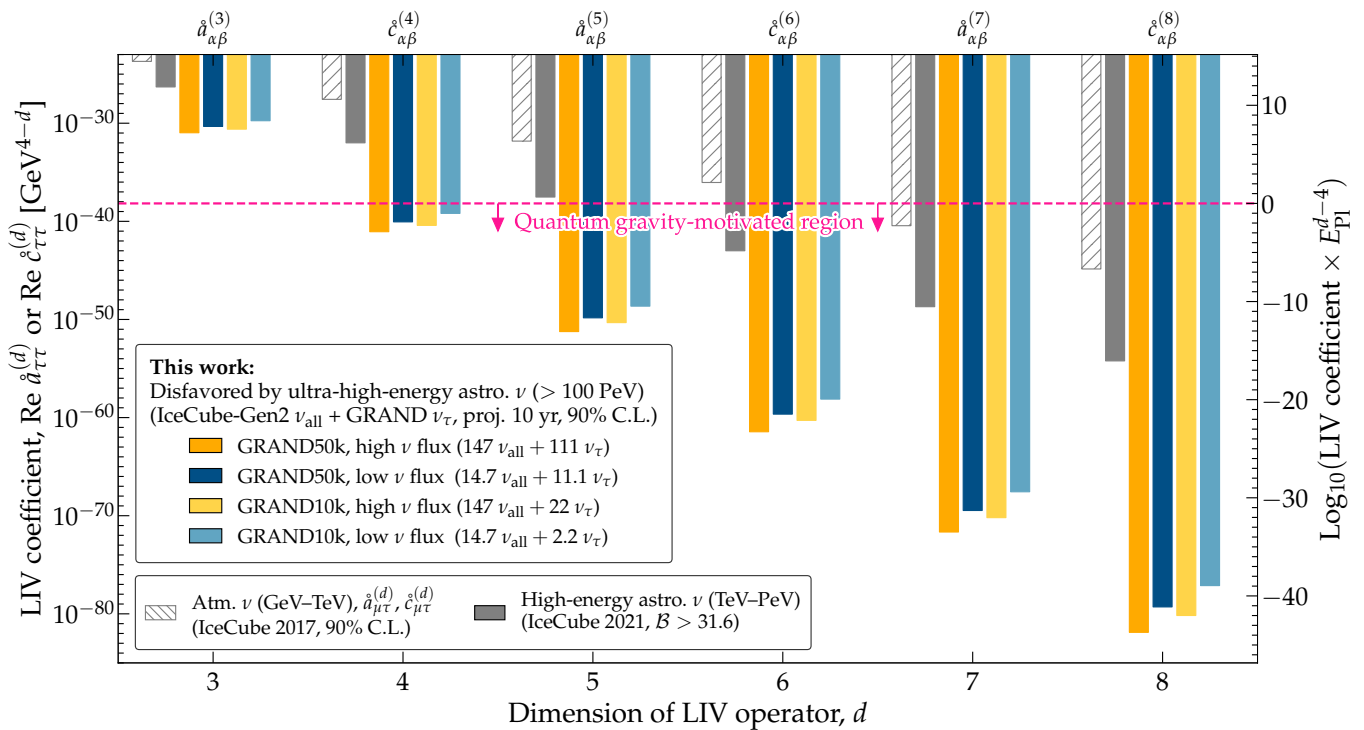


FIG. 4. *Projected limits on LIV from UHE neutrinos.* Our limits come from combining the detection of neutrinos of all flavors by the radio array of IceCube-Gen2 and of ν_τ by GRAND. Limits are on the isotropic LIV coefficients $\hat{a}_{\alpha\beta}^{(d)}$ and $\hat{c}_{\alpha\beta}^{(d)}$ of the Standard Model Extension, which are CPT-odd and CPT-even, respectively. Existing limits come IceCube observations of atmospheric neutrinos [164] (on $\hat{a}_{\mu\tau}^{(d)}$ and $\hat{c}_{\mu\tau}^{(d)}$ instead) and TeV–PeV astrophysical neutrinos [165]. For the latter and our projections, we show limits assuming the canonical flavor composition at the sources, $(\frac{1}{3} : \frac{2}{3} : 0)_S$. Our limits are profiled over the flavor composition at the sources, and the size and shape of the neutrino spectrum.

event rate summed over all flavors, i.e.,

$$\frac{dN^{\text{IC-Gen2}}}{dE_\nu} = \sum_\alpha \frac{dN_\alpha^{\text{IC-Gen2}}}{dE_\nu}, \quad (8)$$

where the contribution of each flavor is computed using Eq. (7) with the flavor-specific effective area.

For GRAND, we start with the effective area of the full-sized array, GRAND200k, reported by the Collaboration in Fig. 25 of Ref. [96]. The effective area is defined for ν_τ only and for detection of neutrinos from 3° – 4° around the horizontal direction, including the contribution of a nearby mountain where neutrinos can interact, i.e., $\Omega = 2\pi(\cos 86^\circ - \cos 93^\circ)$, where the angles are zenith angles measured from the South Pole. For GRAND50k and GRAND10k, we divide the GRAND200k effective area by 4 and 20, respectively. We ignore the potential subdominant contribution of neutrinos of other flavors interacting with the air near the detector [96], since it has not been estimated in detail yet. Thus, for GRAND50k, we use the event rate due to ν_τ only, i.e.,

$$\frac{dN^{\text{GRAND50k}}}{dE_\nu} = \frac{dN_\tau^{\text{GRAND50k}}}{dE_\nu}, \quad (9)$$

computed using Eq. (7) with the effective area of

GRAND50k estimated as outlined above, and similarly for GRAND10k.

Figure 5 shows the mean expected energy distributions of events computed assuming our high benchmark UHE neutrino flux. For each detector, we compute the event rate in the i -th energy bin by integrating the differential event rate over the width of the bin, $\Delta E_{\nu,i}$, i.e.,

$$N_i^{\text{det}} = \int_{\Delta E_{\nu,i}} \frac{dN^{\text{det}}}{dE_\nu} dE_\nu. \quad (10)$$

We use four energy bins per energy decade, evenly spaced in logarithmic scale, from $5 \cdot 10^6$ to $5 \cdot 10^{10}$ GeV for IceCube-Gen2 and from 10^8 to 10^{11} GeV for GRAND, the energy ranges reported in Refs. [96, 107].

IV. MEASURING FLAVOR COMPOSITION

For our high and low benchmark UHE neutrino flux separately, we compute the *true* mean expected number of detected events in IceCube-Gen2 and GRAND, $\bar{\mu}_{\text{IC-Gen2}}$ and $\bar{\mu}_{\text{GRAND}}$. Then, for *test* fluxes, i.e., for test values of the shape parameters $\theta \equiv (\Phi_0, w, E_{\text{bump}})$ and the flavor composition $\mathbf{f}_\oplus \equiv (f_{e,\oplus}, f_{\mu,\oplus}, f_{\tau,\oplus})$

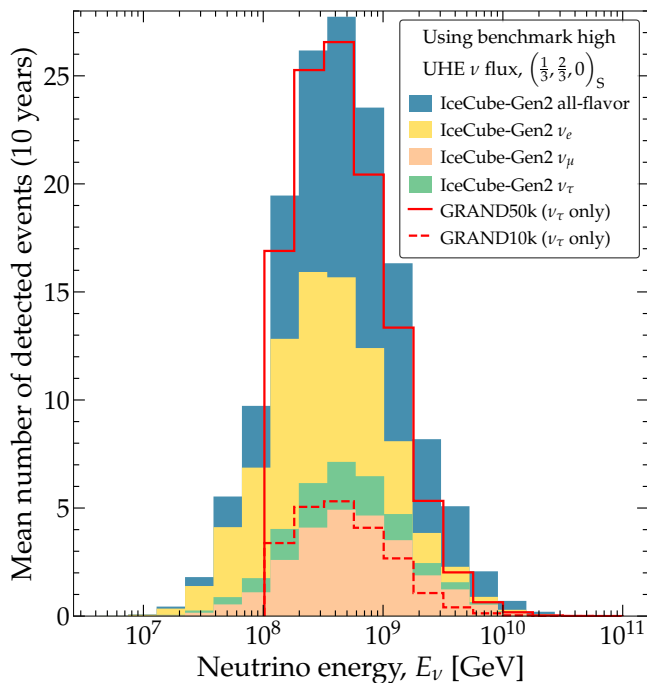


FIG. 5. *Mean expected number of detected events in the radio array of IceCube-Gen2 and GRAND.* In this plot, event rates are computed assuming our benchmark high UHE neutrino flux introduced in the main text. For our benchmark low flux, the event rates (not shown) are ten times smaller. The bin sizes are the same for both detectors, but their positions are slightly different because the energy ranges of IceCube-Gen2 and GRAND that we use are different.

in Eq. (1), we compute the mean expected numbers, $\mu_{\text{IC-Gen2}}(\mathbf{f}_{\oplus}, \boldsymbol{\theta})$ and $\mu_{\text{GRAND}}(\mathbf{f}_{\oplus}, \boldsymbol{\theta})$. We compare Asimov event samples—the mean true *vs.* test rates—in each bin in each experiment via Poisson likelihood functions, and combine them into a total likelihood, i.e.,

$$\ln \mathcal{L}(\mathbf{f}_{\oplus}, \boldsymbol{\theta}) = \sum_{\text{exp}} \sum_i^{\text{bins}} [\bar{\mu}_{i,\text{exp}} \ln \mu_{i,\text{exp}}(\mathbf{f}_{\oplus}, \boldsymbol{\theta}) - \mu_{i,\text{exp}}(\mathbf{f}_{\oplus}, \boldsymbol{\theta})], \quad (11)$$

where $\text{exp} \in \{\text{IC-Gen2}, \text{GRAND}\}$. We build our test statistic by minimizing the likelihood over the flux shape parameters, i.e., $\Lambda(\mathbf{f}_{\oplus}) = 2 [\min_{\boldsymbol{\theta}} \ln \mathcal{L}(\mathbf{f}_{\oplus}, \boldsymbol{\theta}) - \ln \bar{\mathcal{L}}]$, where $\bar{\mathcal{L}}$ is Eq. (11) computed with $\mu_{i,\text{IC-Gen2}}(\mathbf{f}_{\oplus}, \boldsymbol{\theta}) \rightarrow \bar{\mu}_{i,\text{IC-Gen2}}$ and $\mu_{i,\text{GRAND}}(\mathbf{f}_{\oplus}, \boldsymbol{\theta}) \rightarrow \bar{\mu}_{i,\text{GRAND}}$. Wilks' theorem ensures that Λ follows a χ^2 distribution with two degrees of freedom, which we choose to be $f_{e,\oplus}$ and $f_{\mu,\oplus}$ (because $f_{\tau,\oplus} \equiv 1 - f_{e,\oplus} - f_{\mu,\oplus}$, it is not independent). We constrain $f_{e,\oplus}$ and $f_{\mu,\oplus}$ at the 68% and 95% confidence level (C.L.) by demanding $\Lambda = 2.28$ and 6, respectively.

Figure 1 shows the resulting allowed regions of flavor composition at Earth. The allowed regions are roughly aligned with the $f_{\tau,\oplus}$ axis, since this is the predominant flavor fraction extracted from combining IceCube-Gen2

and GRAND. The misalignment comes from IceCube-Gen2 being slightly more sensitive to ν_e than to the other flavors [175] because they are more likely to trigger radio-emitting electromagnetic showers; this is what allows us to disfavor values of $f_{e,\oplus}$ that differ significantly from its true value of about $\frac{1}{3}$, especially those higher.

If the flux is high, the true flavor composition, from pion decay, can be distinguished from the muon-damped one at nearly 95% C.L. and from neutron decay at more than that. If the flux is low, the three benchmarks become indistinguishable at 68% C.L. *Prima facie*, this flavor sensitivity is scant—but it is only deceptively so. Below, we show that, combined with a sensible assumption on ν_{τ} production, it yields ample insight into astrophysics and fundamental physics.

A. Flavor composition at the sources

Knowledge of the flavor composition at Earth allows us to infer the flavor composition with which neutrinos are produced at their sources (S), $f_{\alpha,S}$, averaged over all contributing sources, by undoing the effects of neutrino oscillations. This could allow us to distinguish between competing neutrino production mechanisms [61, 66, 76].

Following Ref. [61] (see also Refs. [66, 76]), we infer the flavor composition at the sources by computing the same test statistic as above, but as a function of $\mathbf{f}_{\alpha,S} \equiv (f_{e,S}, f_{\mu,S}, f_{\tau,S})$, i.e., $\mathcal{L}(\mathbf{f}_S, \boldsymbol{\theta}) = \mathcal{L}[\mathbf{f}_{\oplus}(\mathbf{f}_S), \boldsymbol{\theta}]$, where \mathbf{f}_{\oplus} is obtained from \mathbf{f}_S as indicated earlier. We make two reasonable assumptions. First, we ignore uncertainties in the mixing parameters since by the year 2040 they should be known precisely enough to render the effect of their uncertainty on \mathbf{f}_{\oplus} negligible [66]. Second, we assume that there is no UHE ν_{τ} production, so that we need only infer $f_{e,S}$, since in that case $f_{\mu,S} \equiv 1 - f_{e,S}$; this reduces the likelihood to a single degree of freedom. This is justified because ν_{τ} come from the decay of charmed mesons, whose production is suppressed [178–180].

Figure 3 shows that our projections are promising. Using our high benchmark flux, the true value of $f_{e,S} = 1/3$ is inferred with enough precision to separate it from the alternative muon-damped and neutron-decay compositions at more than 95% C.L. and 99.7% C.L., respectively. Using our low flux, the separation worsens, but remains significant against neutron decay. Similar conclusions hold when using GRAND10k and when assuming $(0 : 1 : 0)_S$ as true instead; see Appendix A.

Distinguishing between the pion-decay and muon-damped flavor composition could constrain the magnetic field intensity in the neutrino sources [42, 63, 181] and, indirectly, their identity. Further, since extragalactic magnetic fields are believed to be weak, inferring a flavor composition compatible with muon-damped could hint at the diffuse UHE neutrino flux being of astrophysical rather than cosmogenic origin.

V. LORENTZ-INVARIANCE VIOLATION

Neutrino oscillations en route to Earth may undergo effects beyond the Standard Model that manifest as deviations to the flavor composition compared to the expectation from standard oscillations [9, 12–14, 37, 54, 182]. Lorentz-invariance violation (LIV), postulated in proposals of quantum gravity, is capable of inducing large deviations [19, 36, 46, 47, 54], making it particularly amenable to testing in experiments. So far, there is no evidence for LIV [183], but the strongest limits on it for neutrinos come from measurements of the flavor composition of the IceCube TeV–PeV astrophysical neutrinos [165]. Because the intensity of LIV is expected to grow with neutrino energy—possibly much faster than linearly—using UHE neutrinos promises vast improvement in the discovery and limiting opportunities.

We adopt the LIV treatment from the Standard Model Extension [183–186], an effective field theory that couples neutrinos to spacetime features. Under LIV, neutrinos are affected by a series of new CPT-odd and CPT-even operators, $\hat{a}^{(d)}$ and $\hat{c}^{(d)}$ of dimension d , each a 3×3 matrix in the flavor basis. They modify neutrino mixing via the Hamiltonian $H = H_{\text{std}} + H_{\text{LIV}}$, where $H_{\text{std}} = M^2/(2E_\nu)$ is the standard term that drives oscillations due to the difference in neutrino masses, with $M^2 \equiv (m_1^2, m_2^2, m_3^2)$ and m_i the mass of the i -th mass eigenstate, and

$$H_{\text{LIV}} = \hat{a}^{(3)} - E_\nu \cdot \hat{c}^{(4)} + E_\nu^2 \cdot \hat{a}^{(5)} - E_\nu^3 \cdot \hat{c}^{(6)} + \dots \quad (12)$$

the contribution from LIV. We compute the average flavor-transition probability as before, but using instead the energy-dependent matrix that diagonalizes the total Hamiltonian, $U'(E_\nu, \hat{a}_{\alpha\beta}^{(d)}, \hat{c}_{\alpha\beta}^{(d)})$. Specifically, the mixing probabilities introduced in Sec. II C are changed to

$$P_{\nu_\beta \rightarrow \nu_\alpha}(E_\nu, z, \hat{a}_{\kappa\lambda}^{(d)}, \hat{c}_{\kappa\lambda}^{(d)}) = \sum_i |U'_{\beta i}[E_\nu(1+z)]|^2 |U'_{\alpha i}(E_\nu)|^2. \quad (13)$$

The flavor composition at Earth depends on energy, the redshift at which the neutrino was produced, z , since cosmological expansion dampens the energy, and the LIV coefficients, i.e., $f'_{\alpha\oplus}(E_\nu, z) = \sum_{\beta,i} |U'_{\beta i}[E_\nu(1+z)]|^2 |U'_{\alpha i}(E_\nu)|^2 f_{\beta,S}$. The values of the LIV coefficients are a priori unknown; below, we constrain them. Since we are mostly sensitive to the ν_τ fraction and since from pion decay most of the emitted flux is in ν_μ , we have higher sensitivity to coefficients that inhibit $\nu_\mu \rightarrow \nu_\tau$ oscillations, i.e., $\hat{a}_{e\mu}^{(d)}$, $\hat{a}_{\tau\tau}^{(d)}$, $\hat{a}_{e\tau}^{(d)}$, and $\hat{a}_{\mu\mu}^{(d)}$, and equivalently for $\hat{c}_{\alpha\beta}^{(d)}$.

Figure 1 illustrates the effect of pure- $\tau\tau$ LIV $[(H_{\text{LIV}})_{\tau\tau}]$, with varying strength relative to standard oscillations $[(H_{\text{std}})_{\tau\tau}]$, on our three flavor-composition benchmarks. Under weak LIV, we recover standard oscillations. Under dominant LIV, ν_τ mixing is suppressed in our simplified scenario where $(H_{\text{LIV}})_{\tau\tau}$ is the only

nonzero LIV component. In-between, interference between the standard and LIV contributions creates the wiggles seen in Fig. 1.

A. Constraints on LIV

We compute the diffuse flux of UHE neutrinos at Earth under LIV from a nondescript population of sources distributed in redshift. The flux is normalized to match our low or high benchmark fluxes. We assume neutrino production via pion decay, i.e., $(\frac{1}{3}, \frac{2}{3}, 0)_S$ (but marginalize over $f_{\alpha,S}$ later). Since the number of LIV coefficients is large, we turn on a single one at a time; in the main text, this is either $\hat{a}_{\tau\tau}^{(d)}$ or $\hat{c}_{\tau\tau}^{(d)}$. To forecast constraints on them, we compute the expected event rates at IceCube-Gen2 and GRAND, and use a test statistic similar to the one introduced earlier, modified to yield upper limits [187], with a likelihood like Eq. (11) but now also dependent on the LIV coefficient, e.g., $\mathcal{L}(\hat{a}_{\tau\tau}^{(d)}, \mathbf{f}_S, \boldsymbol{\theta})$. Like before, we profile over \mathbf{f}_S and $\boldsymbol{\theta}$, and assume no ν_τ production. In Appendix B we provide results for different coefficients.

Figure 4 shows our resulting limits for operators of dimension 3–8. Even in the most pessimistic scenario—low neutrino flux and using GRAND10k—all of our projected limits are better than the present ones [165] by orders of magnitude, since H_{LIV} grows with energy. The relative improvement grows increasingly faster than linearly [Eq. (12)]. This is particularly dramatic for dimension-4 and -5 operators, where our limits reach into the quantum gravity-motivated region, unlike existing limits.

VI. SUMMARY AND OUTLOOK

The near-future discovery of UHE neutrinos, with energies larger than 100 PeV, would bring transformative progress to astrophysics and fundamental physics. Their flavor composition is a particularly versatile probe of both, yet is notoriously difficult to measure, since different neutrino flavors make similar signals in the detectors.

We propose a new strategy to measure the UHE flavor composition that does not rely on individual UHE detectors having flavor-identification capabilities. Combining the indistinct detection of all flavors of one detector—in our work, the radio array of IceCube-Gen2—with the innate sensitivity to predominantly ν_τ of another one—in our work, GRAND—begets access to the fraction of UHE ν_τ . This could be achieved even under conservative conditions: even if the neutrino flux is low, with 10–20 events detected in 10 years, and using intermediate versions of GRAND, one fourth or one tenth of its full planned size.

This flavor sensitivity, though limited, is ripe with insight. For astrophysics, it could identify the production mechanism of UHE neutrinos, distinguishing between

benchmark expectations at 95% C.L. or more. For fundamental physics, it could lead to vast improvement in the constraints on Lorentz-invariance violation, emblematic of the power to test other UHE new physics, e.g., secret neutrino interactions and active-sterile neutrino mixing.

Our methods can be applied to other planned detectors, like RNO-G [94], sensitive to all flavors, and POEMMA [102], sensitive to ν_τ . Further, recent work [106] has shown that in-ice radio-based UHE neutrino telescopes may measure the ν_e and $\nu_\mu + \nu_\tau$ fractions. Our methods would break the degeneracy between ν_μ and ν_τ , providing access to the full flavor composition to tap into

its inherent physics potential.

VII. ACKNOWLEDGMENTS

DF and MB are supported by the VILLUM FONDEN under project no. 29388. This work used resources provided by the High Performance Computing Center at the University of Copenhagen. This project has received funding from the European Union's Horizon 2020 research and innovation program under the Marie Skłodowska-Curie Grant Agreement No. 847523 'INTERACTIONS'.

* federico.testagrossa@studenti.unipd.it

† damiano.fiorillo@nbi.ku.dk

‡ mbustamante@nbi.ku.dk

- [1] L. A. Anchordoqui *et al.*, Cosmic Neutrino Pevatrons: A Brand New Pathway to Astronomy, Astrophysics, and Particle Physics, *JHEAp* **1-2**, 1 (2014), arXiv:1312.6587 [astro-ph.HE].
- [2] M. Ahlers and F. Halzen, Opening a New Window onto the Universe with IceCube, *Prog. Part. Nucl. Phys.* **102**, 73 (2018), arXiv:1805.11112 [astro-ph.HE].
- [3] L. A. Anchordoqui, Ultra-High-Energy Cosmic Rays, *Phys. Rept.* **801**, 1 (2019), arXiv:1807.09645 [astro-ph.HE].
- [4] M. Ackermann *et al.*, Astrophysics Uniquely Enabled by Observations of High-Energy Cosmic Neutrinos, *Bull. Am. Astron. Soc.* **51**, 185 (2019), arXiv:1903.04334 [astro-ph.HE].
- [5] P. Mészáros, D. B. Fox, C. Hanna, and K. Murase, Multi-Messenger Astrophysics, *Nature Rev. Phys.* **1**, 585 (2019), arXiv:1906.10212 [astro-ph.HE].
- [6] F. Halzen and A. Kheirandish, Multimessenger Search for the Sources of Cosmic Rays Using Cosmic Neutrinos, *Front. Astron. Space Sci.* **6**, 32 (2019).
- [7] A. Palladino, M. Spurio, and F. Vissani, Neutrino Telescopes and High-Energy Cosmic Neutrinos, *Universe* **6**, 30 (2020), arXiv:2009.01919 [astro-ph.HE].
- [8] R. Alves Batista *et al.*, EuCAPT White Paper: Opportunities and Challenges for Theoretical Astroparticle Physics in the Next Decade, (2021), arXiv:2110.10074 [astro-ph.HE].
- [9] M. Ackermann *et al.*, High-energy and ultra-high-energy neutrinos: A Snowmass white paper, *JHEAp* **36**, 55 (2022), arXiv:2203.08096 [hep-ph].
- [10] C. Guépin, K. Kotera, and F. Oikonomou, High-energy neutrino transients and the future of multi-messenger astronomy, *Nature Rev. Phys.* **4**, 697 (2022), arXiv:2207.12205 [astro-ph.HE].
- [11] T. K. Gaisser, F. Halzen, and T. Stanev, Particle astrophysics with high-energy neutrinos, *Phys. Rept.* **258**, 173 (1995), [Erratum: *Phys.Rept.* 271, 355–356 (1996)], arXiv:hep-ph/9410384.
- [12] M. Ahlers, K. Helbing, and C. Pérez de los Heros, Probing Particle Physics with IceCube, *Eur. Phys. J. C* **78**, 924 (2018), arXiv:1806.05696 [astro-ph.HE].
- [13] C. A. Argüelles, M. Bustamante, A. Kheirandish, S. Palomares-Ruiz, J. Salvadó, and A. C. Vincent, Fundamental physics with high-energy cosmic neutrinos today and in the future, *PoS ICRC2019*, 849 (2020), arXiv:1907.08690 [astro-ph.HE].
- [14] M. Ackermann *et al.*, Fundamental Physics with High-Energy Cosmic Neutrinos, *Bull. Am. Astron. Soc.* **51**, 215 (2019), arXiv:1903.04333 [astro-ph.HE].
- [15] J. P. Rachen and P. Meszaros, Photohadronic neutrinos from transients in astrophysical sources, *Phys. Rev. D* **58**, 123005 (1998), arXiv:astro-ph/9802280.
- [16] H. Athar, M. Jezabek, and O. Yasuda, Effects of neutrino mixing on high-energy cosmic neutrino flux, *Phys. Rev. D* **62**, 103007 (2000), arXiv:hep-ph/0005104.
- [17] R. M. Crocker, F. Melia, and R. R. Volkas, Searching for long wavelength neutrino oscillations in the distorted neutrino spectrum of galactic supernova remnants, *Astrophys. J. Suppl.* **141**, 147 (2002), arXiv:astro-ph/0106090.
- [18] J. F. Beacom, N. F. Bell, D. Hooper, S. Pakvasa, and T. J. Weiler, Decay of High-Energy Astrophysical Neutrinos, *Phys. Rev. Lett.* **90**, 181301 (2003), arXiv:hep-ph/0211305.
- [19] G. Barenboim and C. Quigg, Neutrino observatories can characterize cosmic sources and neutrino properties, *Phys. Rev. D* **67**, 073024 (2003), arXiv:hep-ph/0301220.
- [20] J. F. Beacom, N. F. Bell, D. Hooper, S. Pakvasa, and T. J. Weiler, Measuring flavor ratios of high-energy astrophysical neutrinos, *Phys. Rev. D* **68**, 093005 (2003), [Erratum: *Phys. Rev. D* 72, 019901 (2005)], arXiv:hep-ph/0307025.
- [21] J. F. Beacom, N. F. Bell, D. Hooper, J. G. Learned, S. Pakvasa, and T. J. Weiler, PseudoDirac neutrinos: A Challenge for neutrino telescopes, *Phys. Rev. Lett.* **92**, 011101 (2004), arXiv:hep-ph/0307151.
- [22] J. F. Beacom, N. F. Bell, D. Hooper, S. Pakvasa, and T. J. Weiler, Sensitivity to θ_{13} and δ in the decaying astrophysical neutrino scenario, *Phys. Rev. D* **69**, 017303 (2004), arXiv:hep-ph/0309267.
- [23] J. F. Beacom and J. Candia, Shower power: Isolating the prompt atmospheric neutrino flux using electron neutrinos, *JCAP* **11**, 009, arXiv:hep-ph/0409046.
- [24] P. D. Serpico, Probing the 2-3 leptonic mixing at high-energy neutrino telescopes, *Phys. Rev. D* **73**, 047301 (2006), arXiv:hep-ph/0511313.
- [25] T. Kashti and E. Waxman, Flavoring astrophysical neutrinos: Flavor ratios depend on energy, *Phys. Rev. Lett.* **95**, 181101 (2005), arXiv:astro-ph/0507599.

- [26] O. Mena, I. Mocioiu, and S. Razzaque, Oscillation effects on high-energy neutrino fluxes from astrophysical hidden sources, *Phys. Rev. D* **75**, 063003 (2007), [arXiv:astro-ph/0612325](#).
- [27] M. Kachelrieß and R. Tomàs, High energy neutrino yields from astrophysical sources I: Weakly magnetized sources, *Phys. Rev. D* **74**, 063009 (2006), [arXiv:astro-ph/0606406](#).
- [28] P. Lipari, M. Lusignoli, and D. Meloni, Flavor Composition and Energy Spectrum of Astrophysical Neutrinos, *Phys. Rev. D* **75**, 123005 (2007), [arXiv:0704.0718 \[astro-ph\]](#).
- [29] S. Pakvasa, W. Rodejohann, and T. J. Weiler, Flavor Ratios of Astrophysical Neutrinos: Implications for Precision Measurements, *JHEP* **02**, 005, [arXiv:0711.4517 \[hep-ph\]](#).
- [30] A. Esmaili and Y. Farzan, An Analysis of Cosmic Neutrinos: Flavor Composition at Source and Neutrino Mixing Parameters, *Nucl. Phys. B* **821**, 197 (2009), [arXiv:0905.0259 \[hep-ph\]](#).
- [31] S. Choubey and W. Rodejohann, Flavor Composition of UHE Neutrinos at Source and at Neutrino Telescopes, *Phys. Rev. D* **80**, 113006 (2009), [arXiv:0909.1219 \[hep-ph\]](#).
- [32] A. Esmaili, Pseudo-Dirac Neutrino Scenario: Cosmic Neutrinos at Neutrino Telescopes, *Phys. Rev. D* **81**, 013006 (2010), [arXiv:0909.5410 \[hep-ph\]](#).
- [33] A. Bhattacharya, S. Choubey, R. Gandhi, and A. Watanabe, Diffuse Ultra-High Energy Neutrino Fluxes and Physics Beyond the Standard Model, *Phys. Lett. B* **690**, 42 (2010), [arXiv:0910.4396 \[hep-ph\]](#).
- [34] S. Hümmer, M. Maltoni, W. Winter, and C. Yaguna, Energy dependent neutrino flavor ratios from cosmic accelerators on the Hillas plot, *Astropart. Phys.* **34**, 205 (2010), [arXiv:1007.0006 \[astro-ph.HE\]](#).
- [35] A. Bhattacharya, S. Choubey, R. Gandhi, and A. Watanabe, Ultra-high neutrino fluxes as a probe for non-standard physics, *JCAP* **09**, 009, [arXiv:1006.3082 \[hep-ph\]](#).
- [36] M. Bustamante, A. M. Gago, and C. Peña-Garay, Energy-Independent New Physics in the Flavour Ratios of High-Energy Astrophysical Neutrinos, *JHEP* **04**, 066, [arXiv:1001.4878 \[hep-ph\]](#).
- [37] P. Mehta and W. Winter, Interplay of energy dependent astrophysical neutrino flavor ratios and new physics effects, *JCAP* **03**, 041, [arXiv:1101.2673 \[hep-ph\]](#).
- [38] P. Baerwald, M. Bustamante, and W. Winter, Neutrino Decays over Cosmological Distances and the Implications for Neutrino Telescopes, *JCAP* **10**, 020, [arXiv:1208.4600 \[astro-ph.CO\]](#).
- [39] L. Fu, C. M. Ho, and T. J. Weiler, Cosmic Neutrino Flavor Ratios with Broken ν_μ - ν_τ Symmetry, *Phys. Lett. B* **718**, 558 (2012), [arXiv:1209.5382 \[hep-ph\]](#).
- [40] S. Pakvasa, A. Joshipura, and S. Mohanty, Explanation for the low flux of high energy astrophysical muon-neutrinos, *Phys. Rev. Lett.* **110**, 171802 (2013), [arXiv:1209.5630 \[hep-ph\]](#).
- [41] A. Chatterjee, M. M. Devi, M. Ghosh, R. Moharana, and S. K. Raut, Probing CP violation with the first three years of ultrahigh energy neutrinos from IceCube, *Phys. Rev. D* **90**, 073003 (2014), [arXiv:1312.6593 \[hep-ph\]](#).
- [42] W. Winter, Photohadronic Origin of the TeV-PeV Neutrinos Observed in IceCube, *Phys. Rev. D* **88**, 083007 (2013), [arXiv:1307.2793 \[astro-ph.HE\]](#).
- [43] X.-J. Xu, H.-J. He, and W. Rodejohann, Constraining Astrophysical Neutrino Flavor Composition from Leptonic Unitarity, *JCAP* **12**, 039, [arXiv:1407.3736 \[hep-ph\]](#).
- [44] E. Aeikens, H. Päs, S. Pakvasa, and P. Sicking, Flavor ratios of extragalactic neutrinos and neutrino shortcuts in extra dimensions, *JCAP* **10**, 005, [arXiv:1410.0408 \[hep-ph\]](#).
- [45] A. Palladino, G. Pagliaroli, F. L. Villante, and F. Visani, What is the Flavor of the Cosmic Neutrinos Seen by IceCube?, *Phys. Rev. Lett.* **114**, 171101 (2015), [arXiv:1502.02923 \[astro-ph.HE\]](#).
- [46] C. A. Argüelles, T. Katori, and J. Salvadó, New Physics in Astrophysical Neutrino Flavor, *Phys. Rev. Lett.* **115**, 161303 (2015), [arXiv:1506.02043 \[hep-ph\]](#).
- [47] M. Bustamante, J. F. Beacom, and W. Winter, Theoretically palatable flavor combinations of astrophysical neutrinos, *Phys. Rev. Lett.* **115**, 161302 (2015), [arXiv:1506.02645 \[astro-ph.HE\]](#).
- [48] G. Pagliaroli, A. Palladino, F. L. Villante, and F. Visani, Testing nonradiative neutrino decay scenarios with IceCube data, *Phys. Rev. D* **92**, 113008 (2015), [arXiv:1506.02624 \[hep-ph\]](#).
- [49] I. M. Shoemaker and K. Murase, Probing BSM Neutrino Physics with Flavor and Spectral Distortions: Prospects for Future High-Energy Neutrino Telescopes, *Phys. Rev. D* **93**, 085004 (2016), [arXiv:1512.07228 \[astro-ph.HE\]](#).
- [50] P. F. de Salas, R. A. Lineros, and M. Tórtola, Neutrino propagation in the galactic dark matter halo, *Phys. Rev. D* **94**, 123001 (2016), [arXiv:1601.05798 \[astro-ph.HE\]](#).
- [51] M. C. González-García, M. Maltoni, I. Martínez-Soler, and N. Song, Non-standard neutrino interactions in the Earth and the flavor of astrophysical neutrinos, *Astropart. Phys.* **84**, 15 (2016), [arXiv:1605.08055 \[hep-ph\]](#).
- [52] M. Bustamante, J. F. Beacom, and K. Murase, Testing decay of astrophysical neutrinos with incomplete information, *Phys. Rev. D* **95**, 063013 (2017), [arXiv:1610.02096 \[astro-ph.HE\]](#).
- [53] D. Biehl, A. Fedynitch, A. Palladino, T. J. Weiler, and W. Winter, Astrophysical Neutrino Production Diagnostics with the Glashow Resonance, *JCAP* **01**, 033, [arXiv:1611.07983 \[astro-ph.HE\]](#).
- [54] R. W. Rasmussen, L. Lechner, M. Ackermann, M. Kowalski, and W. Winter, Astrophysical neutrinos flavored with Beyond the Standard Model physics, *Phys. Rev. D* **96**, 083018 (2017), [arXiv:1707.07684 \[hep-ph\]](#).
- [55] U. K. Dey, D. Kar, M. Mitra, M. Spannowsky, and A. C. Vincent, Searching for Leptoquarks at IceCube and the LHC, *Phys. Rev. D* **98**, 035014 (2018), [arXiv:1709.02009 \[hep-ph\]](#).
- [56] M. Bustamante and S. K. Agarwalla, Universe's Worth of Electrons to Probe Long-Range Interactions of High-Energy Astrophysical Neutrinos, *Phys. Rev. Lett.* **122**, 061103 (2019), [arXiv:1808.02042 \[astro-ph.HE\]](#).
- [57] Y. Farzan and S. Palomares-Ruiz, Flavor of cosmic neutrinos preserved by ultralight dark matter, *Phys. Rev. D* **99**, 051702 (2019), [arXiv:1810.00892 \[hep-ph\]](#).
- [58] M. Ahlers, M. Bustamante, and S. Mu, Unitarity Bounds of Astrophysical Neutrinos, *Phys. Rev. D* **98**, 123023 (2018), [arXiv:1810.00893 \[astro-ph.HE\]](#).
- [59] V. Brdar and R. S. L. Hansen, IceCube Flavor Ratios with Identified Astrophysical Sources: Towards Improving New Physics Testability, *JCAP* **02**, 023,

- arXiv:1812.05541 [hep-ph].
- [60] A. Palladino, The flavor composition of astrophysical neutrinos after 8 years of IceCube: an indication of neutron decay scenario?, *Eur. Phys. J. C* **79**, 500 (2019), arXiv:1902.08630 [astro-ph.HE].
- [61] M. Bustamante and M. Ahlers, Inferring the flavor of high-energy astrophysical neutrinos at their sources, *Phys. Rev. Lett.* **122**, 241101 (2019), arXiv:1901.10087 [astro-ph.HE].
- [62] M. Ahlers, M. Bustamante, and N. G. N. Willesen, Flavors of astrophysical neutrinos with active-sterile mixing, *JCAP* **07**, 029, arXiv:2009.01253 [hep-ph].
- [63] M. Bustamante and I. Tamborra, Using high-energy neutrinos as cosmic magnetometers, *Phys. Rev. D* **102**, 123008 (2020), arXiv:2009.01306 [astro-ph.HE].
- [64] S. Karmakar, S. Pandey, and S. Rakshit, Astronomy with energy dependent flavour ratios of extragalactic neutrinos, *JHEP* **10**, 004, arXiv:2010.07336 [hep-ph].
- [65] D. F. G. Fiorillo, G. Mangano, S. Morisi, and O. Pisanti, IceCube constraints on violation of equivalence principle, *JCAP* **04**, 079, arXiv:2012.07867 [hep-ph].
- [66] N. Song, S. W. Li, C. A. Argüelles, M. Bustamante, and A. C. Vincent, The Future of High-Energy Astrophysical Neutrino Flavor Measurements, *JCAP* **04**, 054, arXiv:2012.12893 [hep-ph].
- [67] B. Telalovic and M. Bustamante, Flavor Anisotropy in the High-Energy Astrophysical Neutrino Sky, (2023), arXiv:2310.15224 [astro-ph.HE].
- [68] M. G. Aartsen *et al.* (IceCube), First observation of PeV-energy neutrinos with IceCube, *Phys. Rev. Lett.* **111**, 021103 (2013), arXiv:1304.5356 [astro-ph.HE].
- [69] M. G. Aartsen *et al.* (IceCube), Evidence for High-Energy Extraterrestrial Neutrinos at the IceCube Detector, *Science* **342**, 1242856 (2013), arXiv:1311.5238 [astro-ph.HE].
- [70] M. G. Aartsen *et al.* (IceCube), Observation of High-Energy Astrophysical Neutrinos in Three Years of IceCube Data, *Phys. Rev. Lett.* **113**, 101101 (2014), arXiv:1405.5303 [astro-ph.HE].
- [71] M. G. Aartsen *et al.* (IceCube), A combined maximum-likelihood analysis of the high-energy astrophysical neutrino flux measured with IceCube, *Astrophys. J.* **809**, 98 (2015), arXiv:1507.03991 [astro-ph.HE].
- [72] M. G. Aartsen *et al.* (IceCube), Evidence for Astrophysical Muon Neutrinos from the Northern Sky with IceCube, *Phys. Rev. Lett.* **115**, 081102 (2015), arXiv:1507.04005 [astro-ph.HE].
- [73] M. G. Aartsen *et al.* (IceCube), Observation and Characterization of a Cosmic Muon Neutrino Flux from the Northern Hemisphere using six years of IceCube data, *Astrophys. J.* **833**, 3 (2016), arXiv:1607.08006 [astro-ph.HE].
- [74] R. U. Abbasi *et al.* (IceCube), The IceCube high-energy starting event sample: Description and flux characterization with 7.5 years of data, *Phys. Rev. D* **104**, 022002 (2021), arXiv:2011.03545 [astro-ph.HE].
- [75] R. U. Abbasi *et al.* (IceCube), Improved Characterization of the Astrophysical Muon-neutrino Flux with 9.5 Years of IceCube Data, *Astrophys. J.* **928**, 50 (2022), arXiv:2111.10299 [astro-ph.HE].
- [76] O. Mena, S. Palomares-Ruiz, and A. C. Vincent, Flavor Composition of the High-Energy Neutrino Events in IceCube, *Phys. Rev. Lett.* **113**, 091103 (2014), arXiv:1404.0017 [astro-ph.HE].
- [77] S. Palomares-Ruiz, A. C. Vincent, and O. Mena, Spectral analysis of the high-energy IceCube neutrinos, *Phys. Rev. D* **91**, 103008 (2015), arXiv:1502.02649 [astro-ph.HE].
- [78] M. G. Aartsen *et al.* (IceCube), Flavor Ratio of Astrophysical Neutrinos above 35 TeV in IceCube, *Phys. Rev. Lett.* **114**, 171102 (2015), arXiv:1502.03376 [astro-ph.HE].
- [79] A. Palladino and F. Vissani, The natural parameterization of cosmic neutrino oscillations, *Eur. Phys. J. C* **75**, 433 (2015), arXiv:1504.05238 [hep-ph].
- [80] A. C. Vincent, S. Palomares-Ruiz, and O. Mena, Analysis of the 4-year IceCube high-energy starting events, *Phys. Rev. D* **94**, 023009 (2016), arXiv:1605.01556 [astro-ph.HE].
- [81] M. G. Aartsen *et al.* (IceCube), Measurements using the inelasticity distribution of multi-TeV neutrino interactions in IceCube, *Phys. Rev. D* **99**, 032004 (2019), arXiv:1808.07629 [hep-ex].
- [82] R. Abbasi *et al.* (IceCube), Detection of astrophysical tau neutrino candidates in IceCube, *Eur. Phys. J. C* **82**, 1031 (2022), arXiv:2011.03561 [hep-ex].
- [83] V. S. Berezinsky and G. T. Zatsepin, Cosmic rays at ultrahigh-energies (neutrino?), *Phys. Lett. B* **28**, 423 (1969).
- [84] M. G. Aartsen *et al.* (IceCube), Differential limit on the extremely-high-energy cosmic neutrino flux in the presence of astrophysical background from nine years of IceCube data, *Phys. Rev. D* **98**, 062003 (2018), arXiv:1807.01820 [astro-ph.HE].
- [85] A. Aab *et al.* (Pierre Auger), Probing the origin of ultrahigh-energy cosmic rays with neutrinos in the EeV energy range using the Pierre Auger Observatory, *JCAP* **10**, 022, arXiv:1906.07422 [astro-ph.HE].
- [86] R. Mammen Abraham *et al.*, Tau neutrinos in the next decade: from GeV to EeV, *J. Phys. G* **49**, 110501 (2022), arXiv:2203.05591 [hep-ph].
- [87] V. B. Valera, M. Bustamante, and C. Glaser, The ultrahigh-energy neutrino-nucleon cross section: measurement forecasts for an era of cosmic EeV-neutrino discovery, *JHEP* **06**, 105, arXiv:2204.04237 [hep-ph].
- [88] D. F. G. Fiorillo, M. Bustamante, and V. B. Valera, Near-future discovery of point sources of ultra-high-energy neutrinos, *JCAP* **03**, 026, arXiv:2205.15985 [astro-ph.HE].
- [89] V. B. Valera, M. Bustamante, and C. Glaser, Near-future discovery of the diffuse flux of ultrahigh-energy cosmic neutrinos, *Phys. Rev. D* **107**, 043019 (2023), arXiv:2210.03756 [astro-ph.HE].
- [90] D. F. G. Fiorillo, V. B. Valera, M. Bustamante, and W. Winter, Searches for dark matter decay with ultrahigh-energy neutrinos endure backgrounds, *Phys. Rev. D* **108**, 103012 (2023), arXiv:2307.02538 [astro-ph.HE].
- [91] V. B. Valera, M. Bustamante, and O. Mena, Joint measurement of the ultra-high-energy neutrino spectrum and cross section, (2023), arXiv:2308.07709 [astro-ph.HE].
- [92] M. G. Aartsen *et al.* (IceCube), The IceCube Neutrino Observatory: Instrumentation and Online Systems, *JINST* **12** (03), P03012, arXiv:1612.05093 [astro-ph.IM].
- [93] M. G. Aartsen *et al.* (IceCube-Gen2), IceCube-Gen2: the window to the extreme Universe, *J. Phys. G* **48**,

- 060501 (2021), arXiv:2008.04323 [astro-ph.HE].
- [94] J. A. Aguilar *et al.* (RNO-G), Design and Sensitivity of the Radio Neutrino Observatory in Greenland (RNO-G), *JINST* **16** (03), P03025, arXiv:2010.12279 [astro-ph.IM].
- [95] J. H. Adams *et al.*, White paper on EUSO-SPB2, (2017), arXiv:1703.04513 [astro-ph.HE].
- [96] J. Álvarez-Muñiz *et al.* (GRAND), The Giant Radio Array for Neutrino Detection (GRAND): Science and Design, *Sci. China Phys. Mech. Astron.* **63**, 219501 (2020), arXiv:1810.09994 [astro-ph.HE].
- [97] C. Deaconu (ANITA), Searches for Ultra-High Energy Neutrinos with ANITA, *PoS ICRC2019*, 867 (2020), arXiv:1908.00923 [astro-ph.HE].
- [98] S. Prohira *et al.*, Observation of Radar Echoes From High-Energy Particle Cascades, *Phys. Rev. Lett.* **124**, 091101 (2020), arXiv:1910.12830 [astro-ph.HE].
- [99] J. Nam *et al.*, High-elevation synoptic radio array for detection of upward moving air-showers, deployed in the Antarctic mountains, *PoS ICRC2019*, 967 (2020).
- [100] S. Wissel *et al.*, Prospects for high-elevation radio detection of >100 PeV tau neutrinos, *JCAP* **11**, 065, arXiv:2004.12718 [astro-ph.IM].
- [101] A. N. Otte, Studies of an air-shower imaging system for the detection of ultrahigh-energy neutrinos, *Phys. Rev. D* **99**, 083012 (2019), arXiv:1811.09287 [astro-ph.IM].
- [102] A. V. Olinto *et al.* (POEMMA), The POEMMA (Probe of Extreme Multi-Messenger Astrophysics) observatory, *JCAP* **06**, 007, arXiv:2012.07945 [astro-ph.IM].
- [103] S.-H. Wang, P. Chen, M. Huang, and J. Nam, Feasibility of Determining Diffuse Ultra-High Energy Cosmic Neutrino Flavor Ratio through ARA Neutrino Observatory, *JCAP* **11**, 062, arXiv:1302.1586 [astro-ph.HE].
- [104] S. Stjärnholm, O. Ericsson, and C. Glaser, Neutrino direction and flavor reconstruction from radio detector data using deep convolutional neural networks, *PoS ICRC2021*, 1055 (2021).
- [105] C. Glaser, D. García-Fernández, and A. Nelles, Prospects for neutrino-flavor physics with in-ice radio detectors, *PoS ICRC2021*, 1231 (2021).
- [106] A. Coleman, O. Ericsson, C. Glaser, and M. Bustamante, Flavor composition of ultrahigh-energy cosmic neutrinos: Measurement forecasts for in-ice radio-based EeV neutrino telescopes, *Phys. Rev. D* **110**, 023044 (2024), arXiv:2402.02432 [astro-ph.HE].
- [107] R. U. Abbasi *et al.* (IceCube-Gen2), Sensitivity studies for the IceCube-Gen2 radio array, *PoS ICRC2021*, 1183 (2021), arXiv:2107.08910 [astro-ph.HE].
- [108] K. Greisen, End to the cosmic ray spectrum?, *Phys. Rev. Lett.* **16**, 748 (1966).
- [109] G. T. Zatsepin and V. A. Kuzmin, Upper limit of the spectrum of cosmic rays, *JETP Lett.* **4**, 78 (1966).
- [110] K. Mannheim, High-energy neutrinos from extragalactic jets, *Astropart. Phys.* **3**, 295 (1995).
- [111] A. M. Atoyan and C. D. Dermer, High-energy neutrinos from photomeson processes in blazars, *Phys. Rev. Lett.* **87**, 221102 (2001), arXiv:astro-ph/0108053.
- [112] A. M. Atoyan and C. D. Dermer, Neutral beams from blazar jets, *Astrophys. J.* **586**, 79 (2003), arXiv:astro-ph/0209231.
- [113] J. Álvarez-Muñiz and P. Mészáros, High energy neutrinos from radio-quiet AGNs, *Phys. Rev. D* **70**, 123001 (2004), arXiv:astro-ph/0409034.
- [114] K. Murase, Y. Inoue, and C. D. Dermer, Diffuse Neutrino Intensity from the Inner Jets of Active Galactic Nuclei: Impacts of External Photon Fields and the Blazar Sequence, *Phys. Rev. D* **90**, 023007 (2014), arXiv:1403.4089 [astro-ph.HE].
- [115] S. S. Kimura, K. Murase, and K. Toma, Neutrino and Cosmic-Ray Emission and Cumulative Background from Radiatively Inefficient Accretion Flows in Low-Luminosity Active Galactic Nuclei, *Astrophys. J.* **806**, 159 (2015), arXiv:1411.3588 [astro-ph.HE].
- [116] P. Padovani, M. Petropoulou, P. Giommi, and E. Resconi, A simplified view of blazars: the neutrino background, *Mon. Not. Roy. Astron. Soc.* **452**, 1877 (2015), arXiv:1506.09135 [astro-ph.HE].
- [117] A. Palladino, X. Rodrigues, S. Gao, and W. Winter, Interpretation of the diffuse astrophysical neutrino flux in terms of the blazar sequence, *Astrophys. J.* **871**, 41 (2019), arXiv:1806.04769 [astro-ph.HE].
- [118] X. Rodrigues, J. Heinze, A. Palladino, A. van Vliet, and W. Winter, Active Galactic Nuclei Jets as the Origin of Ultrahigh-Energy Cosmic Rays and Perspectives for the Detection of Astrophysical Source Neutrinos at EeV Energies, *Phys. Rev. Lett.* **126**, 191101 (2021), arXiv:2003.08392 [astro-ph.HE].
- [119] C. Righi, A. Palladino, F. Tavecchio, and F. Visani, EeV astrophysical neutrinos from flat spectrum radio quasars, *Astron. Astrophys.* **642**, A92 (2020), arXiv:2003.08701 [astro-ph.HE].
- [120] S. S. Kimura, K. Murase, and P. Mészáros, Soft gamma rays from low accreting supermassive black holes and connection to energetic neutrinos, *Nature Commun.* **12**, 5615 (2021), arXiv:2005.01934 [astro-ph.HE].
- [121] A. Neronov and D. Semikoz, Radio-to-Gamma-Ray Synchrotron and Neutrino Emission from Proton-Proton Interactions in Active Galactic Nuclei, *JETP Lett.* **113**, 69 (2021), arXiv:2012.04425 [astro-ph.HE].
- [122] B. Paczynski and G.-H. Xu, Neutrino bursts from gamma-ray bursts, *Astrophys. J.* **427**, 708 (1994).
- [123] E. Waxman and J. N. Bahcall, High-energy neutrinos from cosmological gamma-ray burst fireballs, *Phys. Rev. Lett.* **78**, 2292 (1997), arXiv:astro-ph/9701231.
- [124] K. Murase, K. Ioka, S. Nagataki, and T. Nakamura, High Energy Neutrinos and Cosmic-Rays from Low-Luminosity Gamma-Ray Bursts?, *Astrophys. J. Lett.* **651**, L5 (2006), arXiv:astro-ph/0607104.
- [125] M. Bustamante, P. Baerwald, K. Murase, and W. Winter, Neutrino and cosmic-ray emission from multiple internal shocks in gamma-ray bursts, *Nature Commun.* **6**, 6783 (2015), arXiv:1409.2874 [astro-ph.HE].
- [126] N. Senno, K. Murase, and P. Mészáros, Choked Jets and Low-Luminosity Gamma-Ray Bursts as Hidden Neutrino Sources, *Phys. Rev. D* **93**, 083003 (2016), arXiv:1512.08513 [astro-ph.HE].
- [127] T. Pitik, I. Tamborra, and M. Petropoulou, Neutrino signal dependence on gamma-ray burst emission mechanism, *JCAP* **05**, 034, arXiv:2102.02223 [astro-ph.HE].
- [128] A. Rudolph, M. Petropoulou, W. Winter, and Z. Bošnjak, Multi-messenger Model for the Prompt Emission from GRB 221009A, *Astrophys. J. Lett.* **944**, L34 (2023), arXiv:2212.00766 [astro-ph.HE].
- [129] A. Rudolph, M. Petropoulou, Z. Bošnjak, and W. Winter, Multicollision Internal Shock Lepto-hadronic Models for Energetic Gamma-Ray Bursts (GRBs), *Astrophys. J.* **950**, 28 (2023), arXiv:2212.00765 [astro-

- ph.HE].
- [130] K. Fang, K. Kotera, K. Murase, and A. V. Olinto, Testing the Newborn Pulsar Origin of Ultrahigh Energy Cosmic Rays with EeV Neutrinos, *Phys. Rev. D* **90**, 103005 (2014), [Erratum: *Phys. Rev. D* 92, 129901 (2015)], [arXiv:1311.2044 \[astro-ph.HE\]](#).
- [131] K. Fang, High-Energy Neutrino Signatures of Newborn Pulsars In the Local Universe, *JCAP* **06**, 004, [arXiv:1411.2174 \[astro-ph.HE\]](#).
- [132] G. R. Farrar and A. Gruzinov, Giant AGN Flares and Cosmic Ray Bursts, *Astrophys. J.* **693**, 329 (2009), [arXiv:0802.1074 \[astro-ph\]](#).
- [133] X.-Y. Wang, R.-Y. Liu, Z.-G. Dai, and K. S. Cheng, Probing the tidal disruption flares of massive black holes with high-energy neutrinos, *Phys. Rev. D* **84**, 081301 (2011), [arXiv:1106.2426 \[astro-ph.HE\]](#).
- [134] L. Dai and K. Fang, Can tidal disruption events produce the IceCube neutrinos?, *Mon. Not. Roy. Astron. Soc.* **469**, 1354 (2017), [arXiv:1612.00011 \[astro-ph.HE\]](#).
- [135] N. Senno, K. Murase, and P. Mészáros, High-energy Neutrino Flares from X-Ray Bright and Dark Tidal Disruption Events, *Astrophys. J.* **838**, 3 (2017), [arXiv:1612.00918 \[astro-ph.HE\]](#).
- [136] C. Lunardini and W. Winter, High Energy Neutrinos from the Tidal Disruption of Stars, *Phys. Rev. D* **95**, 123001 (2017), [arXiv:1612.03160 \[astro-ph.HE\]](#).
- [137] B. T. Zhang, K. Murase, F. Oikonomou, and Z. Li, High-energy cosmic ray nuclei from tidal disruption events: Origin, survival, and implications, *Phys. Rev. D* **96**, 063007 (2017), [Addendum: *Phys. Rev. D* 96, 069902 (2017)], [arXiv:1706.00391 \[astro-ph.HE\]](#).
- [138] C. Guépin, K. Kotera, E. Barausse, K. Fang, and K. Murase, Ultra-High Energy Cosmic Rays and Neutrinos from Tidal Disruptions by Massive Black Holes, *Astron. Astrophys.* **616**, A179 (2018), [Erratum: *Astron. Astrophys.* 636, C3 (2020)], [arXiv:1711.11274 \[astro-ph.HE\]](#).
- [139] W. Winter and C. Lunardini, A concordance scenario for the observed neutrino from a tidal disruption event, *Nature Astron.* **5**, 472 (2021), [arXiv:2005.06097 \[astro-ph.HE\]](#).
- [140] W. Winter and C. Lunardini, Interpretation of the Observed Neutrino Emission from Three Tidal Disruption Events, *Astrophys. J.* **948**, 42 (2023), [arXiv:2205.11538 \[astro-ph.HE\]](#).
- [141] R. Aloisio, V. Berezhinsky, and A. Gazizov, Ultra High Energy Cosmic Rays: The disappointing model, *Astropart. Phys.* **34**, 620 (2011), [arXiv:0907.5194 \[astro-ph.HE\]](#).
- [142] K. Kotera, D. Allard, and A. V. Olinto, Cosmogenic Neutrinos: parameter space and detectability from PeV to ZeV, *JCAP* **10**, 013, [arXiv:1009.1382 \[astro-ph.HE\]](#).
- [143] M. Ahlers and F. Halzen, Minimal Cosmogenic Neutrinos, *Phys. Rev. D* **86**, 083010 (2012), [arXiv:1208.4181 \[astro-ph.HE\]](#).
- [144] J. Heinze, D. Boncioli, M. Bustamante, and W. Winter, Cosmogenic Neutrinos Challenge the Cosmic Ray Proton Dip Model, *Astrophys. J.* **825**, 122 (2016), [arXiv:1512.05988 \[astro-ph.HE\]](#).
- [145] K. Fang and K. Murase, Linking High-Energy Cosmic Particles by Black Hole Jets Embedded in Large-Scale Structures, *Nature Phys.* **14**, 396 (2018), [arXiv:1704.00015 \[astro-ph.HE\]](#).
- [146] A. Romero-Wolf and M. Ave, Bayesian Inference Constraints on Astrophysical Production of Ultra-high Energy Cosmic Rays and Cosmogenic Neutrino Flux Predictions, *JCAP* **07**, 025, [arXiv:1712.07290 \[astro-ph.HE\]](#).
- [147] R. Alves Batista, R. M. de Almeida, B. Lago, and K. Kotera, Cosmogenic photon and neutrino fluxes in the Auger era, *JCAP* **01**, 002, [arXiv:1806.10879 \[astro-ph.HE\]](#).
- [148] J. Heinze, A. Fedynitch, D. Boncioli, and W. Winter, A new view on Auger data and cosmogenic neutrinos in light of different nuclear disintegration and air-shower models, *Astrophys. J.* **873**, 88 (2019), [arXiv:1901.03338 \[astro-ph.HE\]](#).
- [149] M. S. Muzio, M. Unger, and G. R. Farrar, Progress towards characterizing ultrahigh energy cosmic ray sources, *Phys. Rev. D* **100**, 103008 (2019), [arXiv:1906.06233 \[astro-ph.HE\]](#).
- [150] A. Anker *et al.* (ARIANNA), White Paper: ARIANNA-200 high energy neutrino telescope, (2020), [arXiv:2004.09841 \[astro-ph.IM\]](#).
- [151] M. S. Muzio, G. R. Farrar, and M. Unger, Probing the environments surrounding ultrahigh energy cosmic ray accelerators and their implications for astrophysical neutrinos, *Phys. Rev. D* **105**, 023022 (2022), [arXiv:2108.05512 \[astro-ph.HE\]](#).
- [152] D. F. G. Fiorillo and M. Bustamante, Bump hunting in the diffuse flux of high-energy cosmic neutrinos, *Phys. Rev. D* **107**, 083008 (2023), [arXiv:2301.00024 \[astro-ph.HE\]](#).
- [153] F. W. Stecker, C. Done, M. H. Salamon, and P. Sommers, High-energy neutrinos from active galactic nuclei, *Phys. Rev. Lett.* **66**, 2697 (1991), [Erratum: *Phys. Rev. Lett.* 69, 2738 (1992)].
- [154] J. G. Learned and K. Mannheim, High-energy neutrino astrophysics, *Ann. Rev. Nucl. Part. Sci.* **50**, 679 (2000).
- [155] W. Winter, Neutrinos from Cosmic Accelerators Including Magnetic Field and Flavor Effects, *Adv. High Energy Phys.* **2012**, 586413 (2012), [arXiv:1201.5462 \[astro-ph.HE\]](#).
- [156] D. F. G. Fiorillo, A. Van Vliet, S. Morisi, and W. Winter, Unified thermal model for photohadronic neutrino production in astrophysical sources, *JCAP* **07**, 028, [arXiv:2103.16577 \[astro-ph.HE\]](#).
- [157] B. Pontecorvo, Inverse beta processes and nonconservation of lepton charge, *Zh. Eksp. Teor. Fiz.* **34**, 247 (1957).
- [158] Z. Maki, M. Nakagawa, and S. Sakata, Remarks on the unified model of elementary particles, *Prog. Theor. Phys.* **28**, 870 (1962).
- [159] I. Esteban, M. C. González-García, M. Maltoni, T. Schwetz, and A. Zhou, The fate of hints: updated global analysis of three-flavor neutrino oscillations, *JHEP* **09**, 178, [arXiv:2007.14792 \[hep-ph\]](#).
- [160] I. Esteban, M. C. González-García, M. Maltoni, T. Schwetz, and A. Zhou, <http://www.nu-fit.org/> (2022), NuFit 5.2.
- [161] N. Aghanim *et al.* (Planck), Planck 2018 results. VI. Cosmological parameters, *Astron. Astrophys.* **641**, A6 (2020), [Erratum: *Astron. Astrophys.* 652, C4 (2021)], [arXiv:1807.06209 \[astro-ph.CO\]](#).
- [162] S. Cole *et al.* (2dFGRS), The 2dF Galaxy Redshift Survey: Near infrared galaxy luminosity functions, *Mon. Not. Roy. Astron. Soc.* **326**, 255 (2001), [arXiv:astro-](#)

- ph/0012429.
- [163] A. M. Hopkins and J. F. Beacom, On the normalisation of the cosmic star formation history, *Astrophys. J.* **651**, 142 (2006), arXiv:astro-ph/0601463.
- [164] M. G. Aartsen *et al.* (IceCube), Neutrino Interferometry for High-Precision Tests of Lorentz Symmetry with IceCube, *Nature Phys.* **14**, 961 (2018), arXiv:1709.03434 [hep-ex].
- [165] R. Abbasi *et al.* (IceCube), Search for quantum gravity using astrophysical neutrino flavour with IceCube, *Nature Phys.* **18**, 1287 (2022), arXiv:2111.04654 [hep-ex].
- [166] F. G. Schröder, Radio detection of Cosmic-Ray Air Showers and High-Energy Neutrinos, *Prog. Part. Nucl. Phys.* **93**, 1 (2017), arXiv:1607.08781 [astro-ph.IM].
- [167] M. G. Aartsen *et al.* (IceCube), Measurement of the multi-TeV neutrino cross section with IceCube using Earth absorption, *Nature* **551**, 596 (2017), arXiv:1711.08119 [hep-ex].
- [168] M. Bustamante and A. Connolly, Extracting the Energy-Dependent Neutrino-Nucleon Cross Section above 10 TeV Using IceCube Showers, *Phys. Rev. Lett.* **122**, 041101 (2019), arXiv:1711.11043 [astro-ph.HE].
- [169] R. Abbasi *et al.* (IceCube), Measurement of the high-energy all-flavor neutrino-nucleon cross section with IceCube, *Phys. Rev. D* **104**, 022001 (2020), arXiv:2011.03560 [hep-ex].
- [170] G. A. Askar'yan, Excess negative charge of an electron-photon shower and its coherent radio emission, *Zh. Eksp. Teor. Fiz.* **41**, 616 (1961).
- [171] F. Halzen, E. Zas, and T. Stanev, Radiodetection of cosmic neutrinos: A Numerical, real time analysis, *Phys. Lett. B* **257**, 432 (1991).
- [172] E. Zas, F. Halzen, and T. Stanev, Electromagnetic pulses from high-energy showers: Implications for neutrino detection, *Phys. Rev. D* **45**, 362 (1992).
- [173] D. Fargion, A. Aiello, and R. Conversano, Horizontal tau air showers from mountains in deep valley: Traces of UHECR neutrino tau, in *26th International Cosmic Ray Conference* (1999) arXiv:astro-ph/9906450.
- [174] F. D. Kahn, I. Lerche, and A. C. B. Lovell, Radiation from cosmic ray air showers <https://doi.org/10.1098/rspa.1966.0007>. (1966).
- [175] J. van Santen, B. A. Clark, R. Halliday, S. Hallmann, and A. Nelles, toise: a framework to describe the performance of high-energy neutrino detectors, *JINST* **17** (08), T08009, arXiv:2202.11120 [astro-ph.IM].
- [176] G. J. Feldman and R. D. Cousins, Unified approach to the classical statistical analysis of small signals, *Physical Review D* **57**, 3873 (1998).
- [177] C. Glaser *et al.*, NuRadioMC: Simulating the radio emission of neutrinos from interaction to detector, *Eur. Phys. J. C* **80**, 77 (2020), arXiv:1906.01670 [astro-ph.IM].
- [178] R. Enberg, M. H. Reno, and I. Sarcevic, High energy neutrinos from charm in astrophysical sources, *Phys. Rev. D* **79**, 053006 (2009), arXiv:0808.2807 [astro-ph].
- [179] J. A. Carpio, K. Murase, M. H. Reno, I. Sarcevic, and A. Stasto, Charm contribution to ultrahigh-energy neutrinos from newborn magnetars, *Phys. Rev. D* **102**, 103001 (2020), arXiv:2007.07945 [astro-ph.HE].
- [180] A. Bhattacharya, R. Enberg, M. H. Reno, and I. Sarcevic, Energy-dependent flavour ratios in neutrino telescopes from charm, (2023), arXiv:2309.09139 [astro-ph.HE].
- [181] S. Hümmer, M. Rüter, F. Spanier, and W. Winter, Simplified models for photohadronic interactions in cosmic accelerators, *Astrophys. J.* **721**, 630 (2010), arXiv:1002.1310 [astro-ph.HE].
- [182] C. A. Argüelles *et al.*, Snowmass white paper: beyond the standard model effects on neutrino flavor: Submitted to the proceedings of the US community study on the future of particle physics (Snowmass 2021), *Eur. Phys. J. C* **83**, 15 (2023), arXiv:2203.10811 [hep-ph].
- [183] V. A. Kostelecky and N. Russell, Data Tables for Lorentz and CPT Violation, *Rev. Mod. Phys.* **83**, 11 (2011), arXiv:0801.0287 [hep-ph].
- [184] D. Colladay and V. A. Kostelecky, Lorentz violating extension of the standard model, *Phys. Rev. D* **58**, 116002 (1998), arXiv:hep-ph/9809521.
- [185] V. A. Kostelecky and M. Mewes, Lorentz and CPT violation in neutrinos, *Phys. Rev. D* **69**, 016005 (2004), arXiv:hep-ph/0309025.
- [186] J. S. Díaz and A. Kostelecky, Lorentz- and CPT-violating models for neutrino oscillations, *Phys. Rev. D* **85**, 016013 (2012), arXiv:1108.1799 [hep-ph].
- [187] G. Cowan, K. Cranmer, E. Gross, and O. Vitells, Asymptotic formulae for likelihood-based tests of new physics, *Eur. Phys. J. C* **71**, 1554 (2011), [Erratum: *Eur. Phys. J. C* **73**, 2501 (2013)], arXiv:1007.1727 [physics.data-an].

Appendix A: Additional plots of flavor composition

To produce our main results, shown in the main text, we use flux benchmarks built assuming a flavor composition at the sources from pion decay, $(\frac{1}{3}, \frac{2}{3}, 0)_S$, and detection in GRAND10k. Below we show results obtained under different assumptions:

Figure 6: Flavor composition at the Earth assuming $(\frac{1}{3}, \frac{2}{3}, 0)_S$ and GRAND10k.

Figure 7: Inferred flavor composition at the sources assuming $(\frac{1}{3}, \frac{2}{3}, 0)_S$ and GRAND10k, i.e., computed from the results in Fig. 6.

Figure 8: Flavor composition at the Earth assuming

muon-damped flavor composition $(0, 1, 0)_S$, and GRAND50k and GRAND10k.

Figure 9: Inferred flavor composition at the sources assuming $(0, 1, 0)_S$, and GRAND50k and GRAND10k, computed from the results in Fig. 8, using the same methods as before [61, 66].

The main observations on and interpretation of Figs. 6–9 are in the main text. Because the flavor composition at Earth for pion-decay and muon-damped production is different, the rates of detected events are different in each case; compare the rates shown in Figs. 1 (in the main text) and 6 *vs.* Figs. 8 and 9.

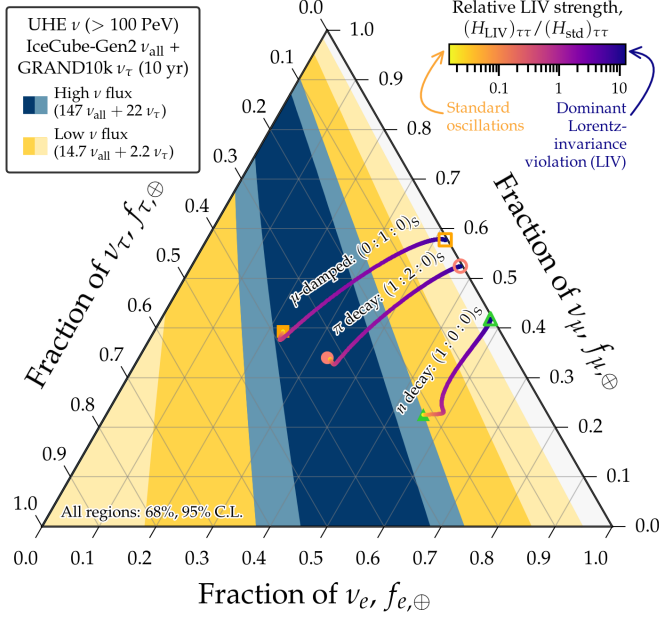


FIG. 6. *Measurement of the UHE neutrino flavor composition at Earth, assuming $(\frac{1}{3}, \frac{2}{3}, 0)_S$ and using GRAND10k.* Same as Fig. 1 in the main text, but for GRAND10k. Figure 7 shows the corresponding inferred flavor composition at the sources.

Appendix B: Results for other LIV operators

In the main text (Fig. 4), we show upper limits on the CPT-odd and CPT-even LIV coefficients $\hat{a}_{\tau\tau}^{(d)}$ and $\hat{c}_{\tau\tau}^{(d)}$, for operators of dimension $d = 3$ to 8. Below we show limits on other LIV coefficients:

Figure 10: Limits on $\hat{a}_{\mu\mu}^{(d)}$ and $\hat{c}_{\mu\mu}^{(d)}$.

Figure 11: Limits on $\hat{a}_{e\mu}^{(d)}$ and $\hat{c}_{e\mu}^{(d)}$.

Figure 12: Limits on $\hat{a}_{e\tau}^{(d)}$ and $\hat{c}_{e\tau}^{(d)}$.

Like for Fig. 4, we show results assuming that the flavor composition at the sources is $(\frac{1}{3}, \frac{2}{3}, 0)_S$, from pion decay. In all cases, our projected limits from UHE neutrinos improve on existing limits. However, for $\hat{a}_{e\tau}^{(d)}$ and $\hat{c}_{e\tau}^{(d)}$, limits are achievable only under the most optimistic scenario, using GRAND50k and our benchmark high neutrino flux because the LIV couplings affect directly only ν_e and ν_τ , which make up the smallest contributions to the flux generated by pion decay.

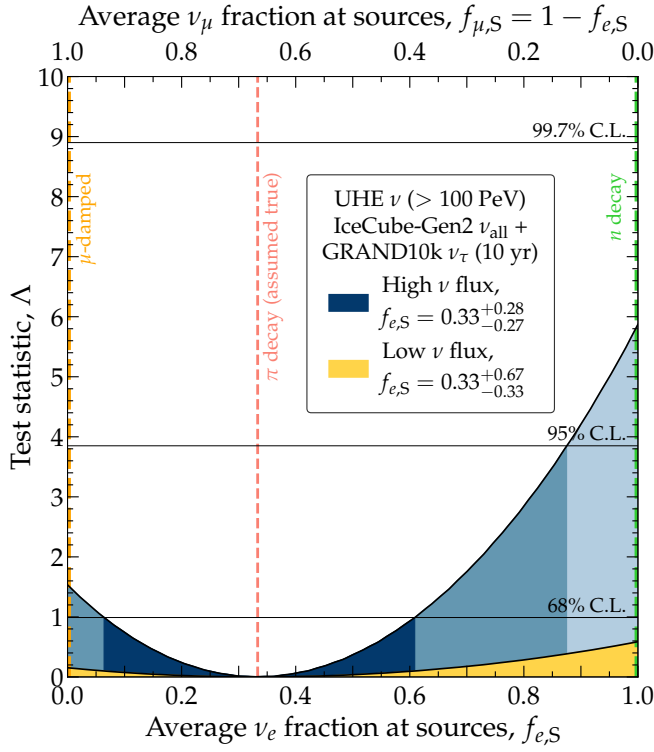


FIG. 7. *Inferred flavor composition of UHE neutrinos at their sources, assuming $(\frac{1}{3}, \frac{2}{3}, 0)_S$, and using GRAND10k.* Same as Fig. 7 in the main text, but for GRAND10k. The results are inferred from the flavor composition at Earth shown in Fig. 6.

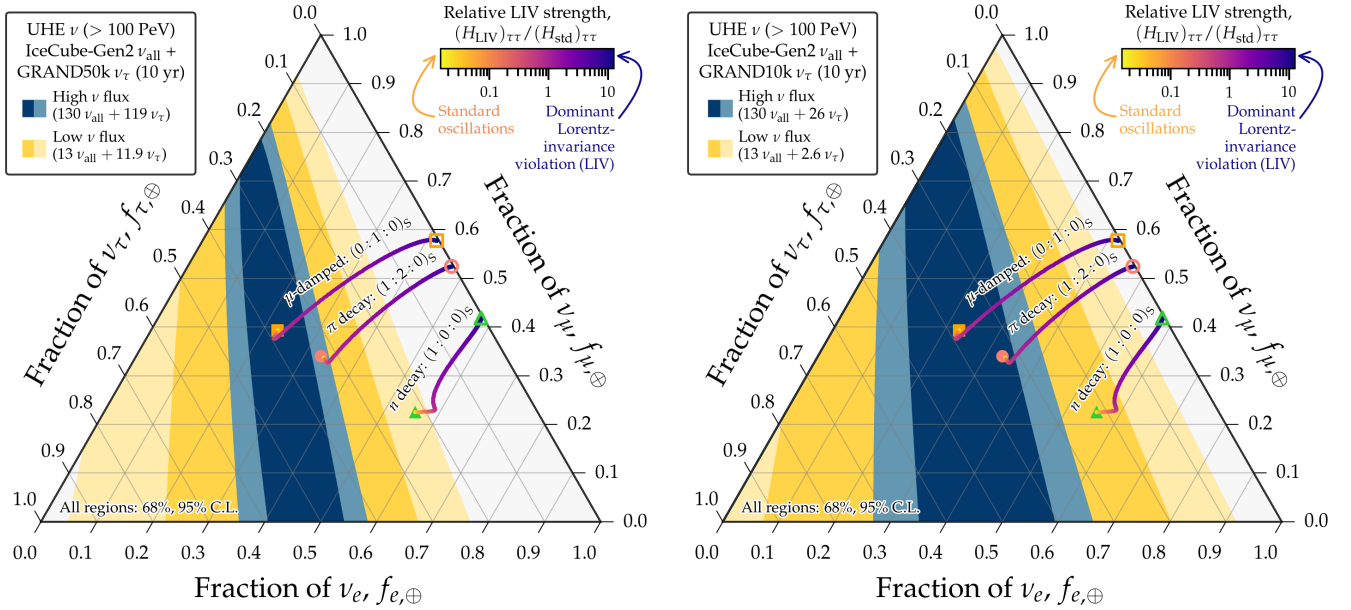


FIG. 8. *Measurement of the UHE neutrino flavor composition at Earth, assuming $(0, 1, 0)_S$.* Left: Using GRAND50k, i.e., same as Fig. 1 in the main text, but for $(0, 1, 0)_S$. Right: Using GRAND10k, i.e., same as Fig. 6, but for $(0, 1, 0)_S$. Figure 9 shows the corresponding inferred flavor composition at the sources.

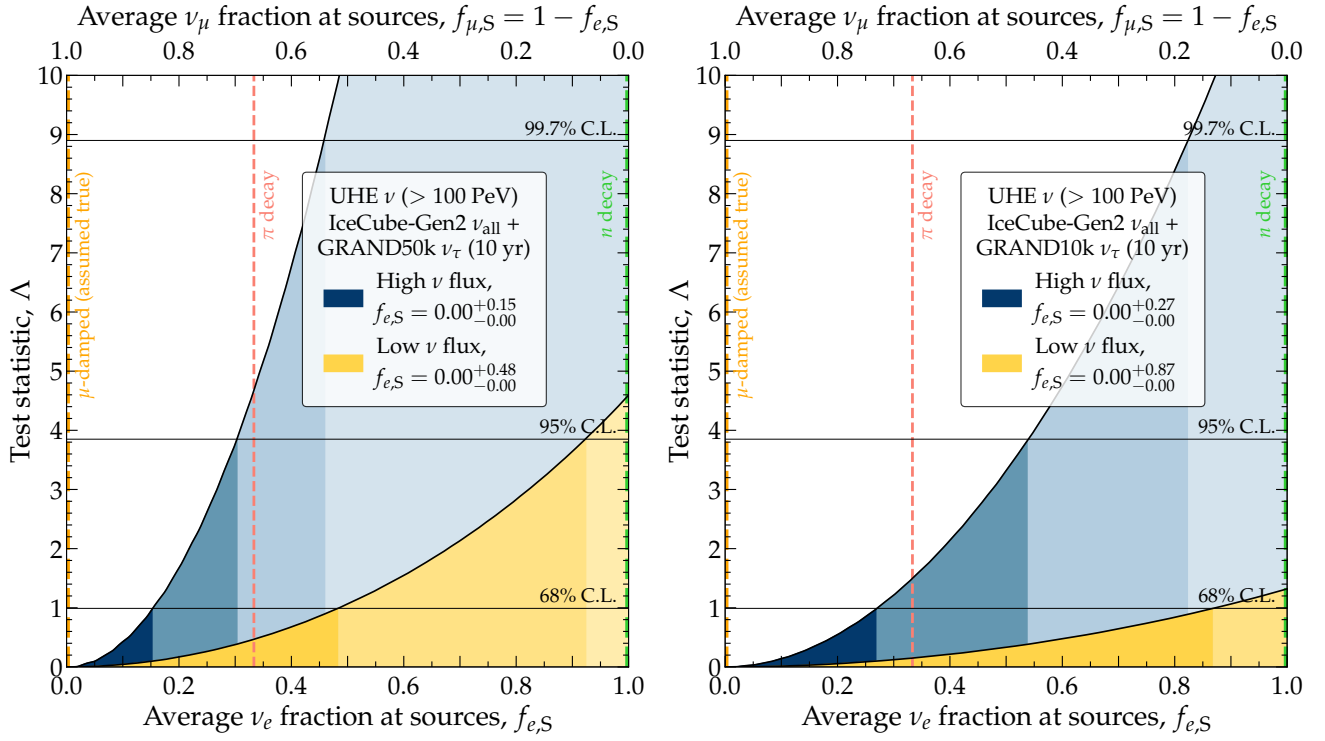


FIG. 9. *Inferred flavor composition of UHE neutrinos at their sources, assuming $(0, 1, 0)_S$. Left: Using GRAND50k, i.e., same as Fig. 3 in the main text, but for $(0, 1, 0)_S$. Right: Using GRAND10k, i.e., same as Fig. 7, but for $(0, 1, 0)_S$.*

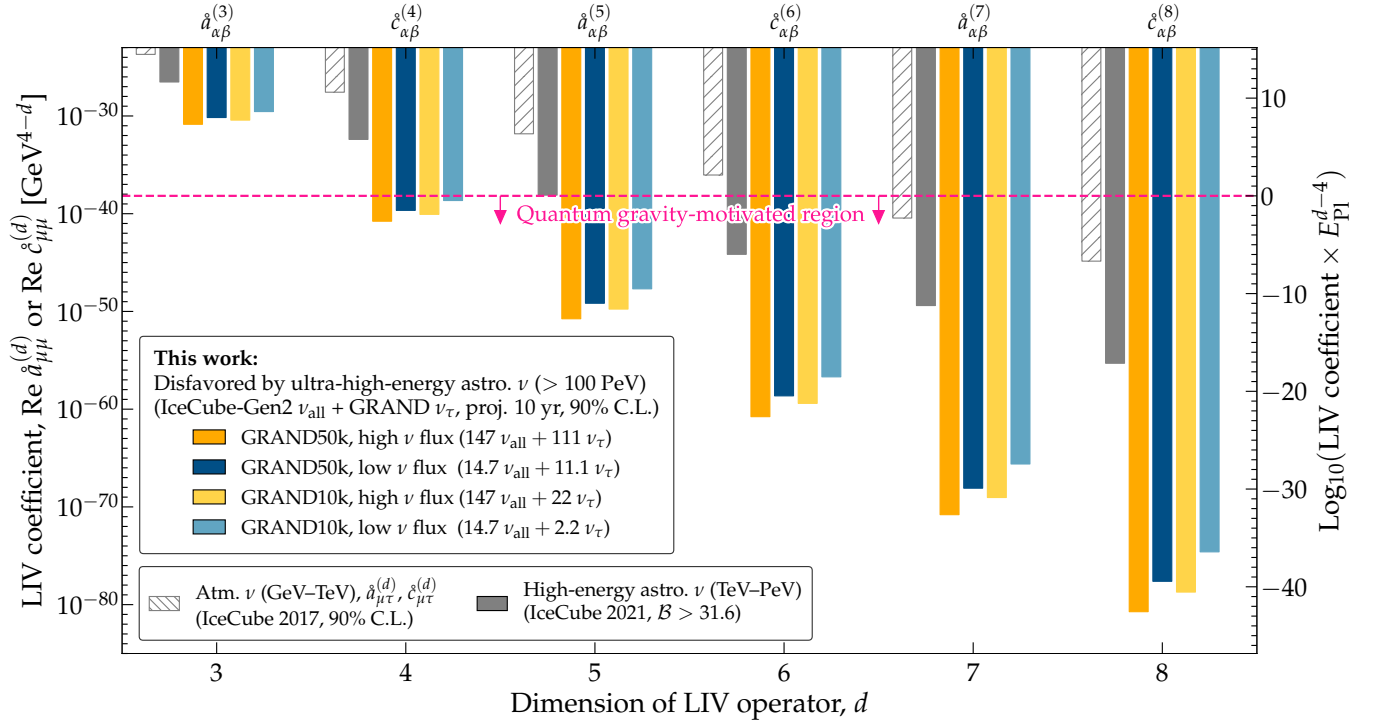


FIG. 10. *Projected limits on LIV coefficients $\hat{a}_{\mu\mu}^{(d)}$ and $\hat{c}_{\mu\mu}^{(d)}$ from UHE neutrinos. Same as Fig. 4 in the main text, but for the $\mu\mu$ LIV coefficients. See Figs. 11 and 12 for other coefficients.*

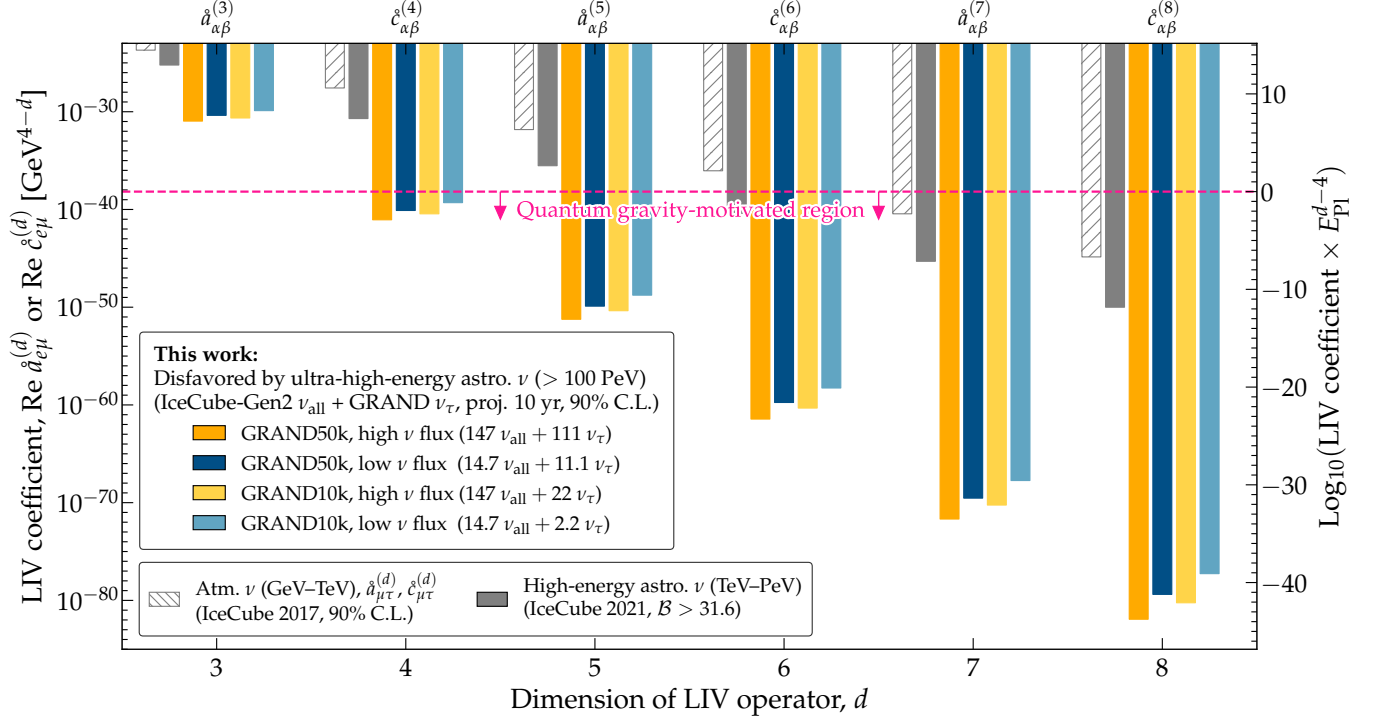


FIG. 11. *Projected limits on LIV coefficients $\hat{a}_{e\mu}^{(d)}$ and $\hat{c}_{e\mu}^{(d)}$ from UHE neutrinos.* Same as Fig. 4 in the main text, but for the $e\mu$ LIV coefficients. See Figs. 12 and 12 for other coefficients.

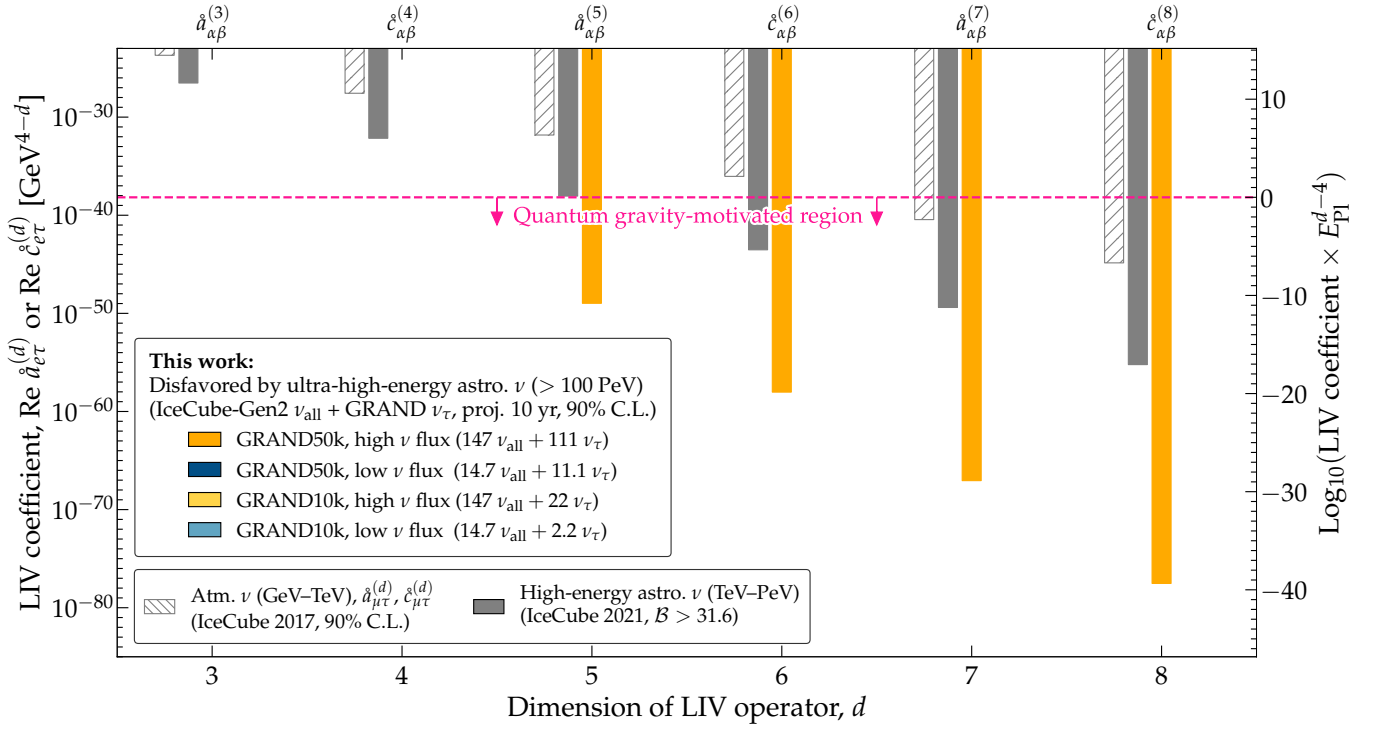


FIG. 12. *Projected limits on LIV coefficients $\hat{a}_{e\tau}^{(d)}$ and $\hat{c}_{e\tau}^{(d)}$ from UHE neutrinos.* Same as Fig. 4 in the main text, but for the $e\tau$ LIV coefficients. Limits are only achievable in the most optimistic scenario, using GRAND50k and our benchmark UHE neutrino flux. See Figs. 10 and 11 for other coefficients.